

phosphite and bromoacetonitrile (Aldrich). The crude product was recrystallized from methanol to give nearly colorless crystals: yield 0.48 g, 80%; mp 70–72 °C; IR (CHCl₃) 2217 (s, CN), 1594 (s, aryl), 1490 (s, aryl) cm⁻¹; ¹H NMR (250 MHz, CDCl₃) δ 2.5 (t, 2 H), 2.7 (t, 2 H), 3.4 (tt, 4 H), 5.2 (s, 1 H), 6.8–6.9 (td, 3 H), 7.3 (t, 2 H); high-resolution MS, found *m/z* 198.1146, calculated for C₁₃H₁₄N₂ *m/z* 198.1157.

1-Phenyl-4-(carboethoxymethylene)piperidine (9) was synthesized on a 3-mmol scale analogous to compound **1** from diethyl carbethoxy-methylphosphonate, which was prepared³² from triethyl phosphite and ethyl bromoacetate (Merck). Purification on a silica gel column yielded a pale yellow oil: yield 0.29 g, 40%; IR (CHCl₃) 1709 (vs, CO), 1600 (vs, aryl), 1579 (m, aryl), 1500 (s, aryl) cm⁻¹; ¹H NMR (250 MHz, CDCl₃) δ 1.3 (t, 3 H), 2.4 (t, 2 H), 3.1 (t, 2 H), 3.3 (tt, 4 H), 4.2 (q, 2 H), 5.7 (s, 1 H), 6.8–6.9 (td, 3 H), 7.3 (t, 2 H); high-resolution MS, found *m/z* 245.1400, calculated for C₁₅H₁₉NO₂ *m/z* 245.1416.

1-Phenyl-4-[(pentafluorophenyl)methylene]piperidine (10) was synthesized on a 1-mmol scale, analogous to compound **1** from diethyl (pentafluorobenzyl)phosphonate, which was prepared³² on a 6.7-mmol scale from triethyl phosphite and pentafluorobenzyl bromide (Aldrich) (yield 83%). Because inferior NaH had been used, only partial reaction occurred. **10** was isolated from the reaction mixture by chromatography (silica gel/chloroform). Recrystallization from ethanol yielded colorless needles: yield 11.2 mg, 3.3%; mp 74–75 °C; IR (CHCl₃) 1594 (m, aryl), 1513 (m, aryl), 1489 (s, aryl), 1132 (m, aryl F) cm⁻¹; ¹H NMR (250 MHz, CDCl₃) δ 2.3 (br t, 2 H), 2.6 (t, 2 H), 3.3 (t, 2 H), 3.4 (t, 2 H), 5.9 (br s, 1 H), 6.8 (t, 1 H), 7.0 (d, 2 H), 7.3 (t, 2 H); high-resolution MS, found *m/z* 339.1048, calculated for C₁₈H₁₄NF₅ *m/z* 339.1046.

1-Phenyl-4-[(3,5-bis(trifluoromethyl)phenyl)methylene]piperidine (11) was synthesized on a 3.08-mmol scale analogous to compound **1** from diethyl 3,5-bis(trifluoromethyl)benzyl phosphonate, which was prepared³² on a 4.3-mmol scale from triethyl phosphite and 3,5-bis(trifluoromethyl)benzyl bromide (Aldrich) (yield 72%). Purification on a silica gel column yielded an off-white solid: yield 150 mg, 9%; mp 62–64 °C; IR (CHCl₃) 1593 (m, aryl), 1490 (m, aryl), 1277 (vs, CF₃) cm⁻¹; ¹H NMR (250 MHz, CDCl₃) δ 2.6 (m, 4 H), 3.3 (t, 2 H), 3.4 (t, 2 H), 6.4 (s, 1 H), 6.9 (t, 1 H), 7.0 (d, 2 H), 7.3 (m, 3 H), 7.65 (s, 1 H), 7.72 (s, 1 H); high-resolution MS, found *m/z* 385.1245, calculated for C₂₀H₁₇NF₆ *m/z* 385.1265.

3.2. Instrumentation. Electronic absorption spectra were recorded on a Hewlett-Packard 8451A diode array spectrophotometer and a Cary 17 D spectrophotometer.

Electronic emission and excitation spectra were recorded on a Spex Fluorolog 2 spectrophotometer.

Cyclic voltammograms were recorded with a Bank Electronic POS 73 Wenking potentiostat coupled to a HP 7090 A measurement plotting system. The reference electrode was Ag/AgCl, saturated KCl (–0.045 V vs SCE³⁵), connected to an acetonitrile solution [electrolyte, tetraethylammonium tetrafluoroborate (0.1 M)] via a 3 M KCl salt bridge (*E*_{ox}(D) = 0.70 V vs SCE³⁶).

(35) Bard, A. J.; Faulkner, L. R. In *Electrochemical Methods*; John Wiley and Sons: New York, 1980.

(36) Meites, L.; Zuman, P. In *Electrochemical Data*; John Wiley and Sons: New York, 1974; Part 1, Vol. A.

Infrared Spectroscopic Studies on the Photocatalytic Hydrogenation of Norbornadiene by Group 6 Metal Carbonyls. 1. The Role of H₂ and the Characterization of Nonclassical Dihydrogen Complexes, (η⁴-Norbornadiene)M(CO)₃(η²-H₂)

Sarah A. Jackson,[†] P. Michael Hodges, Martyn Poliakoff,* James J. Turner, and Friedrich-Wilhelm Grevels[‡]

Contribution from the Department of Chemistry, University of Nottingham, Nottingham, NG7 2RD England, and the Max Planck Institut für Strahlenchemie, D-4330 Mülheim a.d. Ruhr, Federal Republic of Germany. Received June 19, 1989

Abstract: This paper¹ describes the IR characterization of nonclassical H₂ complexes where ethene or norbornadiene (NBD) is coordinated to the *same* d⁶ metal center as the η²-H₂ and discusses the role of such complexes in the photocatalytic hydrogenation of NBD by group 6 metal carbonyl compounds. The dihydrogen complexes are generated in solution by the photolysis of alkene and diene carbonyl complexes in the presence of an overpressure of H₂ or D₂. Photolysis of *trans*-(C₂H₄)₂M(CO)₄ (M = Cr, Mo, and W) (**1**) in liquefied xenon (LXe) doped with H₂ or D₂ at –90 °C leads to the formation of *mer*-(C₂H₄)₂M(CO)₃(H₂) (**2**) (with *trans* C₂H₄ groups) and *cis*-(C₂H₄)M(CO)₄(H₂) (**3**). These species have been characterized by FTIR, and the ν(H–H) IR band of the coordinated η²-H₂ has been detected for the W complexes. All of these compounds react thermally with N₂ to yield the corresponding dinitrogen complexes. Fast (microsecond) time-resolved IR (TRIR) is used to identify *fac*- and *mer*-(NBD)M(CO)₃(*n*-hept) as the primary photoproducts of the photolysis of (NBD)M(CO)₄ [M = Cr, Mo, and W] in *n*-heptane at room temperature. Detailed studies with Mo show that these intermediates react stereospecifically with N₂ and H₂ to give *fac*- and *mer*-(NBD)Mo(CO)₃(X₂) (X₂ = N₂ and H₂). These species can also be generated in LXe by photolysis of either (NBD)Mo(CO)₄ or *mer*-(NBD)Mo(CO)₃(C₂H₄). In addition, photolysis of (NBD)M(CO)₄ [M = Mo or W] in LXe yields products apparently containing η²-NBD, which are not observed in the photolysis at room temperature, probably as a result of differences in temperature and photolysis sources. *fac*-(NBD)Mo(CO)₃(H₂) appears to decay largely by loss of H₂, while *fac*-(NBD)Cr(CO)₃(H₂) and *mer*-(NBD)M(CO)₃(H₂) (M = Cr and Mo) do not decay by this pathway. A mechanism is proposed whereby transfer of H₂ to the diene in *mer*-(NBD)M(CO)₃(H₂) leads to formation of norbornene (NBN) and in *fac*-(NBD)M(CO)₃(H₂) leads to nortricyclene (NTC). The geometries of these two dihydrogen complexes provide a simple rationalization for the observed stereospecificity of the catalytic hydrogenation.

One of the prime examples of photocatalysis is the hydrogenation of dienes in the presence of group 6 transition metal car-

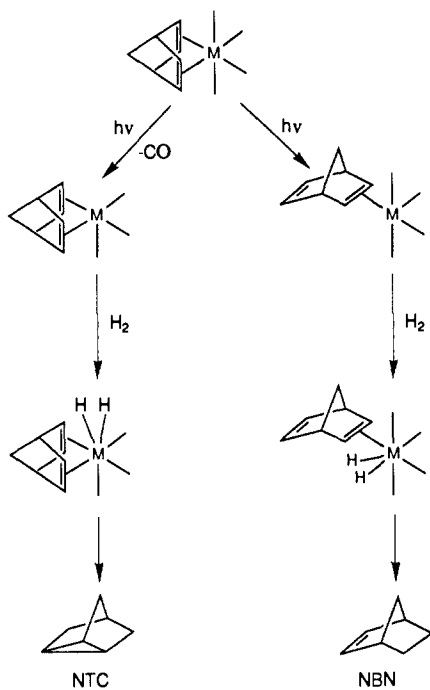
bonyls, M(CO)₆ (M = Cr, Mo, and W).^{2a} The most striking feature of this hydrogenation is that, for conjugated dienes, hy-

[†] Present address: Laboratoire de Chimie Théorique, Université de Paris Sud, 91405 Orsay Cedex, France.

[‡] Max Planck Institut für Strahlenchemie, Mülheim.

(1) Hodges, P. M.; Jackson, S. A.; Jacke, J.; Poliakoff, M.; Turner, J. J.; Grevels, F.-W. *J. Am. Chem. Soc.*, following paper in this issue.

Scheme I



drogenation occurs exclusively at the 1,4-positions. The selectivity and stereospecificity of this catalysis have inspired many workers to study the reaction in detail.² Most of these studies have centered on the hydrogenation of norbornadiene (NBD), where both 1,2- and 1,4-addition occur, giving two possible hydrogenation products, norbornene (NBN) and norbornane (NBN). Darensbourg, in



particular, has made the most concrete proposal for a catalytic cycle³ (Scheme I), which included the suggestion that the catalytic intermediates involve H₂ coordinated *classically* as a dihydride to the same metal center as the diene itself. (In this and subsequent schemes, carbonyl groups are represented by lines without labels; all other ligands are shown explicitly.)

Two significant chemical developments have prompted us to reinvestigate this reaction: (i) the discovery of several nonclassical



H₂ complexes containing η^2 -H₂ coordinated to a d⁶ metal center⁴ and (ii) the isolation and characterization of a wide range of diene and olefin precursor complexes of the group 6 metals.⁵ Con-

currently, there have been a number of spectroscopic developments, particularly the use of liquefied noble gases as cryogenic solvents for stabilizing unstable coordination complexes and the use of time-resolved IR spectroscopy (TRIR) for detecting short-lived reaction intermediates in conventional solutions at room temperature.

The existence of nonclassical H₂ complexes prompts speculation that such H₂ complexes may be key intermediates in hydrogenation processes catalyzed by d⁶ metal carbonyl compounds. If a nonclassical intermediate were involved, the transfer of hydrogen to the organic substrate could occur as a concerted process rather than the more conventional stepwise migration of H atoms.

This is the first of two papers, each highlighting a different aspect of the photocatalytic hydrogenation of dienes. In this paper, we present evidence for the formation of a series of compounds containing either coordinated olefins or dienes and all containing nonclassical H₂ groups bound to the same metal center. These compounds have been detected both in liquid Xe (LXe) at ca. -90 °C and transiently at room temperature. In addition, we use time-resolved IR spectroscopy (TRIR) to detect the primary photoproducts generated in the UV photolysis of (NBD)M(CO)₄. On the basis of these experiments, we propose a mechanism for hydrogenation in which the transfer of H₂ to the diene occurs in the nonclassical (η^4 -NBD)M(CO)₃(η^2 -H₂) complexes.

In the second paper,¹ we use TRIR to monitor the reaction kinetics of "unsaturated" intermediates [e.g. *fac*- and *mer*-(η^4 -NBD)M(CO)₃(*n*-heptane), where the solvent, *n*-heptane, acts as a "token" ligand] and to demonstrate that the reaction of such intermediates with free diene is an integral part of the catalytic process. Using Fourier-transform IR (FTIR) we show that (η^4 -NBD)(η^2 -NBD)M(CO)₃ complexes (M = Mo and W) exist as thermally stable species in the catalytic reaction mixture at room temperature. Finally, we combine the results presented in both papers to present an overall mechanism for the hydrogenation of norbornadiene. Separate papers will detail the synthetic chemistry which has developed in parallel and complements these mechanistic investigations.

Identification of Nonclassical Dihydrogen Complexes

Clearly, a central feature of our studies is the reliable classification of H₂ coordination in mixed diene/H₂ complexes. The coordination mode of dihydrogen can be verified by a variety of techniques including X-ray (or neutron) diffraction,^{4b,6a} NMR T₁ measurements,^{6b} and IR spectroscopy, particularly in liquefied noble gas solution.^{6c-e} In the present case, the catalytic species are unstable and difficult to study by techniques other than IR. However, IR measurements do have an advantage over other spectroscopic methods: not only can η^2 -H₂ frequently be detected directly through the ν (H-H) absorption band but also, in carbonyl complexes, the oxidation state of the metal center can be deduced from the position of the ν (C-O) bands.

In our experiments, dihydrogen complexes are formed by the photochemical substitution of CO or C₂H₄ groups of a metal complex in a solvent doped with H₂. As a result of several studies^{6c-e} involving d⁶ and d¹⁰ metal centers, we have established a set of criteria for identifying nonclassical dihydrogen complexes using IR spectroscopy.

(a) The best IR evidence for the presence of η^2 -H₂ is the observation, in LXe solution, of the IR absorption due to the ν (H-H) stretch^{6c-e} of the η^2 -H₂ group in the region 3100–2600 cm⁻¹. When D₂ is used instead of H₂, this absorption should shift to lower frequency (by ca. 1/√2). However, the ν (H-H) absorption is

(2) (a) Nasielski, J.; Kirsch, P.; Wilputte-Steinert, L. *J. Organomet. Chem.* **1971**, *27*, C13. (b) Platbrood, G.; Wilputte-Steinert, L. *Bull. Soc. Chim. Belg.* **1973**, *82*, 733. (c) Wrighton, M. S.; Schroeder, M. A. *J. Am. Chem. Soc.* **1973**, *95*, 5764. (d) Platbrood, G.; Wilputte-Steinert, L. *J. Organomet. Chem.* **1974**, *70*, 393. (e) *Ibid.* **1974**, *70*, 407. (f) *Tetrahedron Lett.* **1974**, *29*, 2507. (g) *J. Organomet. Chem.* **1975**, *85*, 199. (h) Fischler, I.; Budzwait, M.; Koerner von Gustorf, E. A. *J. Organomet. Chem.* **1976**, *105*, 325.

(3) (a) Darensbourg, D. J.; Nelson, H. H., III. *J. Am. Chem. Soc.* **1974**, *96*, 6511. (b) Darensbourg, D. J.; Nelson, H. H., III; Murphy, M. A. *J. Am. Chem. Soc.* **1977**, *99*, 896.

(4) (a) Kubas, G. J.; Ryan, R. R.; Swanson, B. I.; Vergamini, P. J.; Wasserman, H. J. *J. Am. Chem. Soc.* **1984**, *106*, 451. (b) For excellent reviews, see: Kubas, G. J. *Acc. Chem. Res.* **1988**, *21*, 120. Ginsburg, A. G.; Bagaturyants, A. A. *Metalloorg. Khim.* **1989**, *2*, 249.

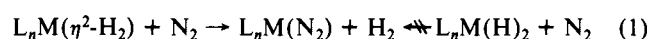
(5) (b) Grevels, F.-W.; Skibbe, V. *J. Chem. Soc., Chem. Commun.* **1984**, 681. (b) Grevels, F.-W.; Jacke, J.; Ozkar, S. *J. Am. Chem. Soc.* **1987**, *109*, 7536. (c) Grevels, F.-W.; Jacke, J.; Klotzbücher, W. E.; Ozkar, S.; Skibbe, V. *Pure Appl. Chem.* **1988**, *60*, 1017.

(6) (a) Morris, R. H.; Sawyer, J. H.; Shiralian, M.; Zubkowski, J. D. *J. Am. Chem. Soc.* **1985**, *107*, 5581. (b) Crabtree, R. H.; Hamilton, D. G. *J. Am. Chem. Soc.* **1986**, *108*, 3124. (c) Upmacis, R. K.; Gadd, G. E.; Poliakov, M.; Simpson, M. B.; Turner, J. J.; Whyman, R.; Simpson, A. F. *J. Chem. Soc., Chem. Commun.* **1985**, 27. (d) Upmacis, R. K.; Poliakov, M.; Turner, J. J. *J. Am. Chem. Soc.* **1986**, *108*, 3645. (e) Gadd, G. E.; Upmacis, R. K.; Poliakov, M.; Turner, J. J. *Ibid.* **1986**, *108*, 2547. (f) Burdett, J. K.; Phillips, J. R.; Poliakov, M.; Pourian, M.; Turner, J. J.; Upmacis, R. K. *Inorg. Chem.* **1987**, *26*, 3054. (g) Kober, E. M.; Hay, P. J. *The Challenge of d and f Electrons*; Salahub, D. R., Zerner, M. C., Eds.; ACS Symposium Series 394; American Chemical Society: Washington, DC, 1989; p 92.

typically very weak, and its detection requires relatively high concentrations of the dihydrogen complex in solution.^{6c} In the work described here, such an absorption has been detected for at least two of the complexes.⁷

(b) The carbonyl bands, $\nu(\text{C}-\text{O})$, of an $\eta^2\text{-H}_2$ complex are comparable in both position and relative intensity to those of the corresponding N_2 complex.⁸ (An $\eta^2\text{-H}_2$ carbonyl metal complex can easily be distinguished from an N_2 carbonyl metal complex because the $\eta^2\text{-H}_2$ complex does not, of course, have IR bands in the $\nu(\text{N}-\text{N})$ region.) By contrast the $\nu(\text{C}-\text{O})$ bands of a dihydride complex would be expected to occur at a higher wavenumber than the bands of the corresponding N_2 complex because of the higher oxidation state of the metal center. In those cases where an equilibrium has been shown to exist between classical and non-classical forms of the same compound, the $\nu(\text{C}-\text{O})$ bands of the classical form have been observed 30–40 cm^{-1} higher than those of the nonclassical form.⁹

(c) Most $\eta^2\text{-H}_2$ complexes,^{4c} including all those which we have studied in LXe, will react thermally with N_2 forming the analogous N_2 complex^{6d,8,10} (eq 1).



The reactions reported in this paper are the first of our experiments where there is a possibility of hydrogenation occurring within the $\eta^2\text{-H}_2$ complexes. It will be shown that, under those conditions, displacement of $\eta^2\text{-H}_2$ by N_2 does not necessarily occur.

Experimental Section

Experiments in Liquefied Noble Gases. The apparatus for experiments in LXe solution has been described extensively elsewhere.¹¹ With high-pressure apparatus (20 atm, 300 psi), LXe can be used as a solvent over the temperature range –110 to ca. –30 °C. The cells (2.4-cm pathlength) have two pairs of opposing windows, one pair (CaF_2) for UV photolysis (250-W high-pressure Hg arc lamp) and a second pair (KRS5) for IR detection. All IR spectra were recorded at 2-cm⁻¹ resolution on a Nicolet MX-3600 FTIR interferometer (16K data points, 32K transform points). Under the conditions of our experiments, a trace impurity of N_2 is usually present at the ppm level, an amount often sufficient to give rise to detectable concentrations of dinitrogen complexes even in the absence of added N_2 . As will be seen, however, this trace contamination can be turned to advantage in the characterization of nonclassical dihydrogen complexes.

Time-Resolved Infrared (TRIR) Spectroscopy. The TRIR apparatus at Nottingham has been previously described.¹² Briefly, it consists of a line-tunable CW CO laser (Edinburgh Instruments PL3 with modified cooling system and diffraction grating, giving a series of narrow lines ca. 4 cm^{-1} apart over a tuning range of 1680–2010 cm^{-1}) as the IR source, a UV excimer laser (Lumonics Hyperex HE-440 operating at 308 nm) as the photolysis source, and a fast infrared detection system. By measuring the change in the IR absorption of the solution following the UV flash at a known wavelength and by repeating this procedure throughout the tuning range of the IR source, a series of point-by-point infrared spectra may be constructed by computer, which correspond to a series of time delays after the flash. Given the spacing of the CO laser lines, the "resolution" of the apparatus¹² is nominally 8 cm^{-1} , but it is possible to distinguish bands closer together than 8 cm^{-1} , provided that the bands are due to two different species which are evolving at different

Table I. Comparison of the Products of the Reaction of $(\text{C}_2\text{H}_4)_2\text{W}(\text{CO})_4$ with H_2 or D_2 in Liquid Xenon at –110 °C

	$\text{X}_2 = \text{H}_2$	$\text{X}_2 = \text{D}_2$	assignment
<i>mer</i> - $(\text{C}_2\text{H}_4)_2\text{W}(\text{CO})_3(\text{X}_2)$	2041.5	2040.3	a' C_s
	1948.8	1948.2	$a' + a''^b$
<i>cis</i> - $(\text{C}_2\text{H}_4)_2\text{W}(\text{CO})_4(\text{X}_2)$	2059.0	2056.8	a' C_s
	1952.6	a	a'
	1939.0	1938.4	a''
	1923.7	1922.7	a'

^a Obscured by parent and other product bands. ^b This band is assigned to two overlapping $\nu(\text{C}-\text{O})$ modes.

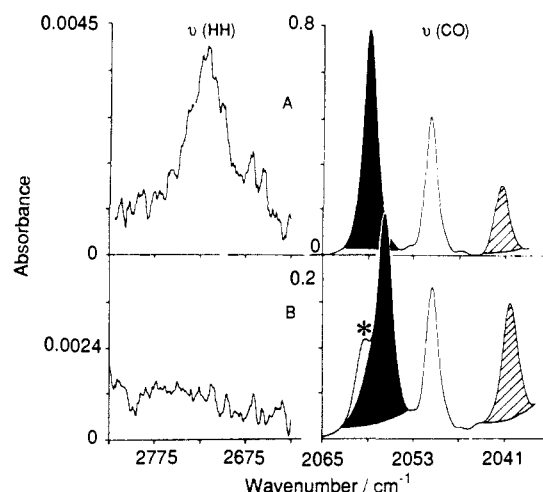


Figure 1. IR spectra in the $\nu(\text{H}-\text{H})$ and part of the $\nu(\text{C}-\text{O})$ region in LXe at –114 °C. Spectrum A shows the products of the photoreaction of $(\text{C}_2\text{H}_4)_2\text{W}(\text{CO})_4$ with H_2 . An absorption in the $\nu(\text{H}-\text{H})$ region can be observed. Spectrum B was taken after subsequent UV photolysis of the same solution but with an added pressure of D_2 . No band in the $\nu(\text{H}-\text{H})$ region is observed. The bands in the $\nu(\text{C}-\text{O})$ region are marked as follows: black, *cis*- $(\text{C}_2\text{H}_4)_2\text{W}(\text{CO})_4(\text{X}_2)$ ($\text{X}_2 = \text{H}_2$ in A and D_2 in B; cross-hatched, *mer*- $(\text{C}_2\text{H}_4)_2\text{W}(\text{CO})_3(\text{X}_2)$ ($\text{X}_2 = \text{H}_2$ in A and D_2 in B; unmarked due to *cis*- $(\text{C}_2\text{H}_4)_2\text{W}(\text{CO})_4(\text{N}_2)$; the asterisk marks residual *cis*- $(\text{C}_2\text{H}_4)_2\text{W}(\text{CO})_4(\text{H}_2)$. (Note that, in this and subsequent figures, the shading of a band is largely to aid visualization and does not necessarily show the exact area of the particular band.)

rates. Recent developments in this apparatus include the use of a new fast infrared detection system comprising a Laser Monitoring Systems photovoltaic MCT detector (Model S-0025; fastest rise time 150 ns) and a Gould 4072 storage oscilloscope. Technical details of kinetic measurements using TRIR will be given in our second paper.¹

Chemicals. All gases were used without further purification: N_2 , H_2 , D_2 (99.99%) (BDH chemicals and Messer Griesheim) and CO and Xe (BOC Research Grade). *n*-Heptane (Aldrich, HPLC grade) was distilled over CaH_2 prior to use. The olefin and diene complexes were synthesized at the Max Planck Institut für Strahlenchemie.

Results and Discussion

General Strategy. Our overall aim has been to demonstrate that the presence of olefin or diene ligands does not alter the propensity of d^6 metal centers to form nonclassical dihydrogen complexes. We have studied the photochemical reactions of *trans*- $(\text{C}_2\text{H}_4)_2\text{M}(\text{CO})_4$ and $(\text{NBD})\text{M}(\text{CO})_4$ ($\text{M} = \text{Cr}, \text{Mo}, \text{or W}$) with N_2 and H_2 in liquid Xe solution and identified nonclassical dihydrogen complexes by use of the criteria listed above. We have also studied the behavior of $(\text{NBD})\text{M}(\text{CO})_4$ at room temperature in conventional solvents, using TRIR to identify intermediates and the products formed by the reaction of these intermediates with H_2 and N_2 . There is excellent agreement between the results in LXe and at room temperature. Although results for all three group 6 metals are summarized in the tables, we only describe each experiment in detail for one metal with brief comments on the behavior of the other two.

Photochemistry of *trans*- $(\text{C}_2\text{H}_4)_2\text{M}(\text{CO})_4$ in Liquid Xe (LXe).
(a) Reaction of *trans*- $(\text{C}_2\text{H}_4)_2\text{W}(\text{CO})_4$ with H_2 . Although the

(7) If D_2 is used in the place of H_2 , one cannot use shifts in the position of the $\nu(\text{C}-\text{O})$ bands as evidence of the bonding mode of H_2 because such shifts are expected for both classical and nonclassical H_2 due to changes in vibrational coupling between $\nu(\text{M}-\text{H})$ and $\nu(\text{C}-\text{O})$ in classical compounds and between $\nu(\text{D}-\text{D})$ and $\nu(\text{C}-\text{O})$ in nonclassical.

(8) Jackson, S. A.; Upmacis, R. K.; Poliakoff, M.; Turner, J. J.; Burdett, J. K.; Grevels, F.-W. *J. Chem. Soc., Chem. Commun.* **1987**, 678.

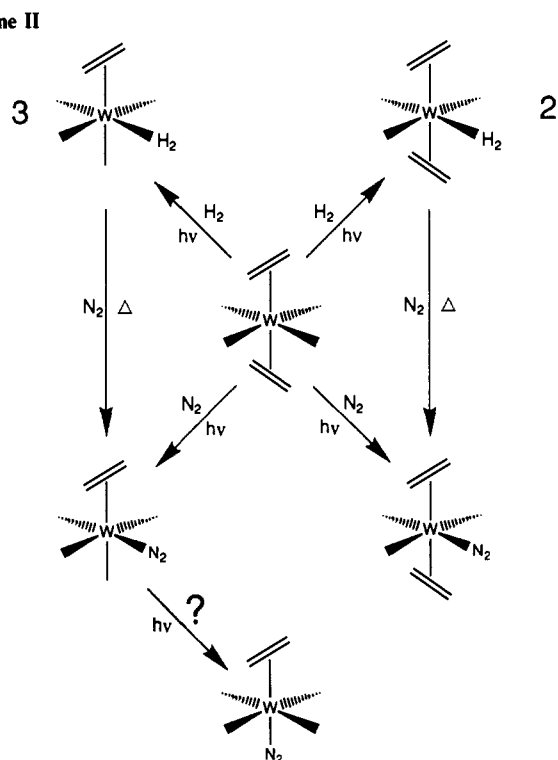
(9) Kubas, G. J.; Unkefer, C. J.; Swanson, B. I.; Fukushima, E. *J. Am. Chem. Soc.* **1986**, *108*, 7000.

(10) Morris, R. H.; Earl, K. A.; Luck, R. L.; Lazarowych, N. J.; Sella, A. *Inorg. Chem.* **1987**, *26*, 2674.

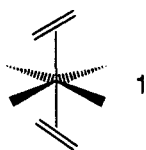
(11) (a) Maier, W. B.; Poliakoff, M.; Simpson, M. B.; Turner, J. J. *J. Mol. Struct.* **1982**, *80*, 83. (b) Turner, J. J.; Poliakoff, M.; Howdle, S. M.; Jackson, S. A.; McLaughlin, J. G. *Faraday Discuss. Chem. Soc.* **1988**, *86*, 271.

(12) Dixon, A. J.; Healy, M. A.; Hodges, P. M.; Moore, B. D.; Poliakoff, M.; Simpson, M. B.; Turner, J. J.; West, M. A. *J. Chem. Soc., Faraday Trans. 2* **1986**, *82*, 2083. Hodges, P. M. Ph.D. Thesis, University of Nottingham, 1988.

Scheme II



complex $\text{trans}-(\text{C}_2\text{H}_4)_2\text{Cr}(\text{CO})_4$ was first observed in LXe solution,¹³ the bis-ethene complexes of all three group 6 metals were subsequently found to be sufficiently stable to be isolated.^{5b} The *trans*-ethene groups adopt an orthogonal conformation,^{5b} 1, and it is this feature that gives the complexes their stability. The complexes are extremely soluble in LXe and their D_{2d} symmetry leads to a single strong $\nu(\text{C}-\text{O})$ band (e) with a weaker band (b_2) to higher frequency. Photolysis of $\text{trans}-(\text{C}_2\text{H}_4)_2\text{W}(\text{CO})_4$ dis-



solved in LXe doped with H_2 generates six new IR bands in the $\nu(\text{C}-\text{O})$ stretching region of the spectrum. These $\nu(\text{C}-\text{O})$ bands, unlike those of other species in the solution, show a small but reproducible shift⁷ when D_2 is used instead of H_2 (see Table I and Figure 1), indicating that the bands are due to products with coordinated H_2 (or D_2). We can make a tentative assignment to two products by comparison with the IR spectra of the corresponding *trans*-cyclooctene complexes.⁸ These products are *mer*- $(\text{C}_2\text{H}_4)_2\text{W}(\text{CO})_3(\text{H}_2)$ (2H_2) (expected $\nu(\text{C}-\text{O})$; $2a' + a''$) and *cis*- $(\text{C}_2\text{H}_4)\text{W}(\text{CO})_4(\text{H}_2)$ (3H_2) (expected $\nu(\text{C}-\text{O})$; $3a' + a''$), which appear to be generated in similar quantities (see Scheme II).

An examination of the rest of the IR spectrum¹⁴ provides more definitive proof that these complexes do indeed contain $\eta^2\text{-H}_2$. A weak band is observed at 2717 cm^{-1} in a region characteristic of the $\nu(\text{H}-\text{H})$ vibration of $\eta^2\text{-H}_2$. Moreover, this band¹⁵ is not

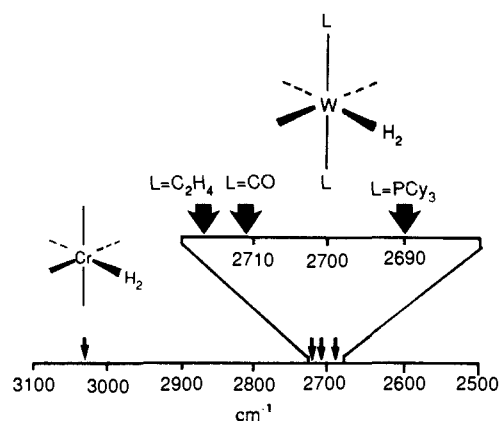


Figure 2. Schematic representation of the positions of the $\nu(\text{H}-\text{H})$ stretches of nonclassical dihydrogen compounds; $\text{W}(\text{CO})_3(\text{PCy}_3)_2(\text{H}_2)$ ⁴ is in a Nujol mull, and $\text{Cr}(\text{CO})_5(\text{H}_2)$,^{6c} $\text{W}(\text{CO})_5(\text{H}_2)$,^{6d} and $(\text{C}_2\text{H}_4)_x\text{W}(\text{CO})_{(5-x)}(\text{H}_2)$ ($x = 1$ or 2) are in LXe.

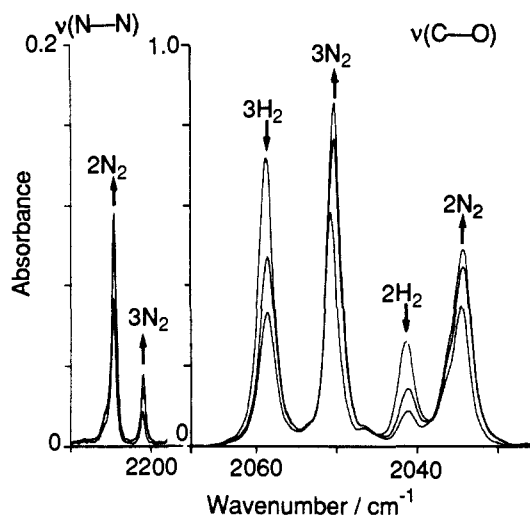


Figure 3. IR spectra in the $\nu(\text{N}-\text{N})$ and part of the $\nu(\text{C}-\text{O})$ regions in LXe solution at $-114\text{ }^\circ\text{C}$ showing the thermal reaction of *mer*- $(\text{C}_2\text{H}_4)_2\text{W}(\text{CO})_3(\text{H}_2)$, marked 2H_2 , and *cis*- $(\text{C}_2\text{H}_4)\text{W}(\text{CO})_4(\text{H}_2)$, marked 3H_2 , with a trace impurity of N_2 (in the presence of 230 psi H_2) to form respectively, *mer*- $(\text{C}_2\text{H}_4)_2\text{W}(\text{CO})_3(\text{N}_2)$, marked 2N_2 , and *cis*- $(\text{C}_2\text{H}_4)\text{W}(\text{CO})_4(\text{N}_2)$, marked 3N_2 . The growths and decays of the bands, which occurred over a period of 1 h, are indicated by arrows.

observed when D_2 is used instead of H_2 ; see Figure 1.

Although the $\nu(\text{C}-\text{O})$ spectra indicate two products containing H_2 , *mer*- $(\text{C}_2\text{H}_4)_2\text{W}(\text{CO})_3(\text{H}_2)$ and *cis*- $(\text{C}_2\text{H}_4)\text{W}(\text{CO})_4(\text{H}_2)$, only a single $\nu(\text{H}-\text{H})$ stretch is observed. The band is, however, somewhat broader, ca. 50 cm^{-1} fwhm, than the $\nu(\text{H}-\text{H})$ band of $\text{W}(\text{CO})_5(\text{H}_2)$ (40 cm^{-1} fwhm under similar conditions^{11b}). It is therefore not unreasonable to assign this band to the overlapping $\nu(\text{H}-\text{H})$ absorptions of the two complexes. This assignment is also supported by the fact that the position of the $\nu(\text{H}-\text{H})$ band, 2717 cm^{-1} , is very close to that of the $\nu(\text{H}-\text{H})$ of both $\text{W}(\text{C}-\text{O})_5(\text{H}_2)$ (2711 cm^{-1})^{6c} and $\text{W}(\text{CO})_3(\text{PCy}_3)_2(\text{H}_2)$ (2690 cm^{-1})^{4a} (see Figure 2). By contrast, the $\nu(\text{H}-\text{H})$ stretches of these $\text{W}-\text{H}_2$ complexes are considerably shifted from the $\nu(\text{H}-\text{H})$ of $\text{Cr}(\text{C}-\text{O})_5(\text{H}_2)$ (3030 cm^{-1}). Thus, the position of the $\nu(\text{H}-\text{H})$ stretch appears to depend predominantly on the metal to which the H_2 is bound; the presence of other ligands seems to have relatively little influence. Further evidence for the presence of $\eta^2\text{-H}_2$ in these species comes from their thermal reaction with traces of N_2 . Once generated, the complexes react thermally with traces of N_2 in the solution¹⁶ (see Figure 3). The products of these reactions can

(13) Gregory, M. F.; Jackson, S. A.; Poliakoff, M.; Turner, J. J. *J. Chem. Soc., Chem. Commun.* **1986**, 1175.

(14) Further examination of the spectrum also shows a new band at 1169 cm^{-1} which can be observed growing in just below a strong band due to 1 (1179 cm^{-1}) which has been assigned to the $\nu(\text{C}=\text{C})$ of coordinated ethylene. The new band may well be the overlapping $\nu(\text{C}=\text{C})$ bands of *mer*- $(\text{C}_2\text{H}_4)_2\text{W}(\text{CO})_3(\text{H}_2)$ and *cis*- $(\text{C}_2\text{H}_4)\text{W}(\text{CO})_4(\text{H}_2)$ shifted down from the parent absorption by 10 cm^{-1} . Our previous work^{11b} has shown that the $\nu(\text{H}-\text{H})$ band of $\text{W}(\text{CO})_5(\text{H}_2)$ has an absorbance ca. 0.02 that of the highest frequency $\nu(\text{C}-\text{O})$ band (a_1). In Figure 1 the $\nu(\text{H}-\text{H})$ band is somewhat weaker relative (0.005) to the highest frequency $\nu(\text{C}-\text{O})$ band of *cis*- $(\text{C}_2\text{H}_4)\text{W}(\text{CO})_4(\text{H}_2)$. This difference is probably not significant; the a_1 bands of $\text{M}(\text{CO})_5\text{L}$ are notoriously weak.

(15) The $\nu(\text{D}-\text{D})$ stretch due to coordinated $\eta^2\text{-D}_2$ should occur around 1900 cm^{-1} and must be obscured by the intense bands in the $\nu(\text{C}-\text{O})$ region.

Table II. Wavenumbers (cm⁻¹) of $\nu(\text{C-O})$ Bands of Mixed Ethene/H₂ and Mixed Ethene/N₂ Complexes in Liquid Xe

	chromium	molybdenum	tungsten	
(C ₂ H ₄) ₂ M(CO) ₄ ^a	1987 ^b	1999 ^c	1996.6 ^b	D _{2d}
	1952	1964	1964	e
mer(C ₂ H ₄) ₂ M(CO) ₃ (D ₂)		2037.2 ^d	2040.3 ^e	C _s
		1947.1	1948.2	a' + a''
mer(C ₂ H ₄) ₂ M(CO) ₃ (N ₂)		2234.9 ^d	2218.7 ^e	$\nu(\text{N-N})$ a'
		2034.5	2034.6	a'
		1949.0	1949.1	a' + a''
cis(C ₂ H ₄)M(CO) ₄ (D ₂)	2049.2 ^e	2057.9 ^d	2056.8 ^e	a'
	f	f	1952.6 ^f	a'
	f	1933.8	1938.4	a''
	1925.1	1924.6	1922.7	a'
cis(C ₂ H ₄)M(CO) ₄ (N ₂)	2223.4 ^e	2229.3 ^d	2204.3 ^e	$\nu(\text{N-N})$ a'
	2043.1	2052.4	2050.9	a'
	f	1955.5	f	a'
	f	1935.6	1935.4	a'
	1929.7	1927.5	1926.2	a'

^a These wavenumbers are less precise since the complexes are so soluble that concentrations were very high and the bands are very intense. ^b LXe at -100 °C. ^c LXe at -91 °C. ^d LXe at -110 °C. ^e LXe at -112 °C. ^f Not observed. ^g Value from H₂ complex; this band is obscured for D₂.

be identified as *mer*-(C₂H₄)₂W(CO)₃(N₂) 2N₂ and *cis*-(C₂H₄)W(CO)₄(N₂) 3N₂ from their $\nu(\text{C-O})$ and $\nu(\text{N-N})$ bands (Table II). These dinitrogen complexes can also be prepared directly by UV photolysis of *trans*-(C₂H₄)₂W(CO)₄ in LXe doped with N₂. Under these photochemical conditions, a third weak $\nu(\text{N-N})$ band was observed at 2172.0 cm⁻¹. No $\nu(\text{C-O})$ bands were observed for this species, presumably because they were obscured by more intense absorptions. This $\nu(\text{N-N})$ band is tentatively assigned to *trans*-(C₂H₄)W(CO)₄(N₂), possibly generated by secondary photolysis.

(b) **Reaction of *trans*-(C₂H₄)₂Mo(CO)₄ with D₂.** Analogous experiments with Mo as the metal center generate the new products, *mer*-(C₂H₄)₂Mo(CO)₃(D₂) and *cis*-(C₂H₄)Mo(CO)₄(D₂) with $\nu(\text{C-O})$ bands similar in position and relative intensity to those of the W compounds (Table II). The Mo complexes, however, are thermally less stable than their W congeners.¹⁷ Nevertheless, the complexes are almost certainly nonclassical in view of their thermal reaction with dinitrogen, which generates products *mer*-(C₂H₄)₂Mo(CO)₃(N₂) and *cis*-(C₂H₄)Mo(CO)₄(N₂) (see Table II). The same complexes can also be generated photochemically by direct reaction of *trans*-(C₂H₄)₂Mo(CO)₄ with N₂.

(c) **Reaction of *trans*-(C₂H₄)₂Cr(CO)₄ with D₂.** The photo-products of the reaction between *trans*-(C₂H₄)₂Cr(CO)₄ and D₂ are so thermally unstable that they can only be observed while the LXe solution is actually being irradiated. Figure 4a shows part of the IR spectrum recorded during 2 min of UV photolysis.

(16) The fact that H₂ rather than N₂ products are observed upon photolysis of the solution is purely a kinetic effect due to the relative concentrations of H₂ and N₂ in the solution. On standing, the thermodynamically more stable N₂ products gradually increase in concentration at the expense of the H₂ species. There is a definite isotope effect in these thermal reactions. The D₂ complexes are somewhat less reactive than their H₂ analogues, as might be expected from differences in zero-point energy. Since the reactions involve trace impurities, kinetic data can only be regarded as qualitative. However, typically, the D₂ complexes took 11 h to decay completely under a 180 psi overpressure of D₂ while a comparable decay of the H₂ species took 1 h 20 min under 200 psi of H₂. The rate of decay is dependent on the pressure of H₂ (or D₂), consistent with the loss of H₂ (D₂) as the rate-determining step.

(17) Only 13 min after the completion of UV photolysis, *mer*-(C₂H₄)₂Mo(CO)₃(D₂) can no longer be detected in LXe solution at -115 °C (180 psi D₂), and the bands of *cis*-(C₂H₄)Mo(CO)₄(D₂) have decayed by about half. Because of this lability, the D₂ complexes cannot be generated in sufficient quantity for detection of $\nu(\text{D-D})$ bands due to $\eta^2\text{-D}_2$. In the chromium system, no *mer*-(C₂H₄)₂Cr(CO)₃(X₂) (X = H or N) complexes have been observed even in LKr but this is presumably because such a product is too unstable to be observed by this method. By contrast, UV photolysis of (C₂H₄)₂Cr(CO)₄ in LXe doped with C₂H₄ provides evidence for the formation of a relatively unstable species, probably *mer*-(C₂H₄)₃Cr(CO)₃: $\nu(\text{C-O})$ 2008.0, 1934.0, and 1929.7 cm⁻¹.

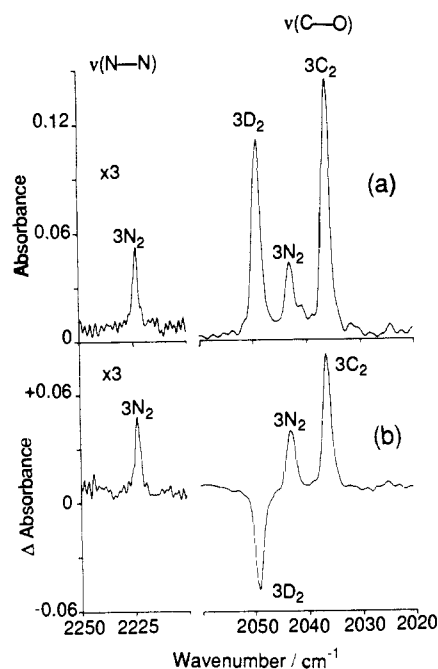
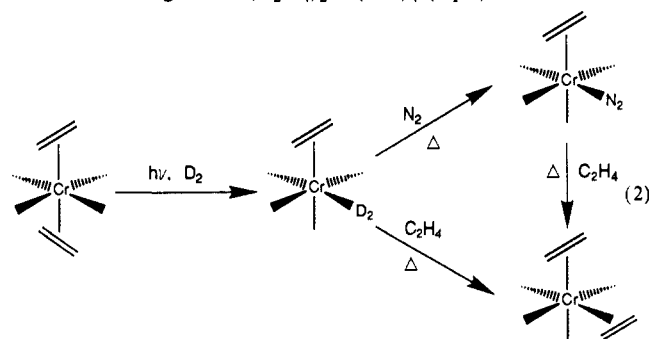


Figure 4. IR spectra in part of the $\nu(\text{C-O})$ and $\nu(\text{N-N})$ regions showing the changes during and after UV photolysis of a LXe solution of (C₂H₄)₂Cr(CO)₄ at -112 °C under a pressure of 200 psi D₂. Spectrum (a) was recorded during UV irradiation. The bands are labeled as follows: 3D₂, *cis*-(C₂H₄)Cr(CO)₄(D₂); 3N₂, *cis*-(C₂H₄)Cr(CO)₄(N₂); 3C₂, *cis*-(C₂H₄)₃Cr(CO)₄. After UV photolysis, there is a rapid thermal reaction of the labile D₂ complex as illustrated by spectrum (b). This is an IR difference spectrum, showing the peaks growing and decaying over a period of 5 min after the lamp is switched off. The peaks are labeled as in spectrum (a).

The only detectable product containing D₂ is *cis*-(C₂H₄)Cr(CO)₄(D₂), the bands of which can be assigned by comparison with the corresponding Mo and W species (Table II). IR bands due to *cis*-(C₂H₄)Cr(CO)₄(N₂) are also observed.

Photolysis also generated the relatively stable species *cis*-(C₂H₄)₂Cr(CO)₄,¹³ presumably by reaction with free ethene in solution. Figure 4b also shows that *cis*-(C₂H₄)Cr(CO)₄(D₂) decays thermally into *cis*-(C₂H₄)Cr(CO)₄(N₂) by reaction with trace N₂ in solution. The N₂ product is also unstable and in turn reacts with ethene to give *cis*-(C₂H₄)₂Cr(CO)₄ (eq 2).



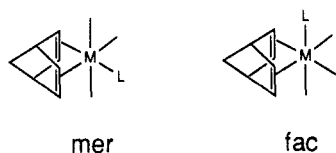
Although (tricyclo)Cr(CO)₅ [tricyclo = *trans*-cyclooctene] is thermally much more stable^{5a} than (C₂H₄)Cr(CO)₅,¹³ all of the mixed C₂H₄/η²-H₂ complexes, described above, are significantly more stable than the corresponding tricyclo/η²-H₂ complexes.⁸ For example, *cis*-(C₂H₄)Cr(CO)₄(D₂) is observable in LXe at -110 °C while *cis*-(tricyclo)Cr(CO)₄(D₂) can only be detected at temperatures less than -120 °C in LKr solution.^{8,18}

(18) Steric arguments are sometimes invoked to explain differences in lability of closely related complexes of weak ligands. For example, steric effects can rationalize the greater reactivity of the *cis* isomer of W(CO)₄L- (*n*-heptane) [L = phosphine or phosphite] compared to the *trans*.²⁰ In the present case, it could be argued that the greater lability of the D₂ in the tricyclo complex is due to the greater steric bulk of tricyclo compared to C₂H₄. However, D₂ is such a small ligand that steric effects may not be the dominant effect.

A feature of all these reactions has been the observation that photolysis of *trans*-(C₂H₄)₂M(CO)₄ generates the product *cis*-(C₂H₄)M(CO)₄(H₂). This is interesting because reaction of a *trans* compound leads to the formation of a *cis* product. Isomerization also plays an important part in the photolysis of (NBD)M(CO)₃(C₂H₄) described below. Similar processes have been observed in a number of other d⁶ systems,^{19,20} where they have been attributed to excited-state rearrangements of coordinatively unsaturated species.

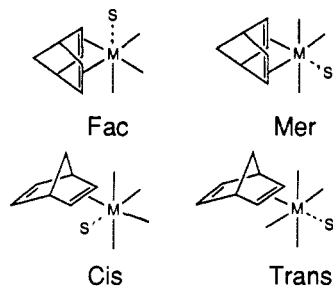
The most significant point of the experiments described above is that they provide evidence for the formation of only nonclassical dihydrogen compounds. Coordination of either one or two ethene groups to a d⁶ metal center does not promote the formation of dihydride species. The next section describes the generation of dihydrogen and dinitrogen species more directly related to the photocatalytic hydrogenation of norbornadiene.

Photochemistry of (Norbornadiene)M(CO)₄. Photolytic substitution of a CO group on (NBD)M(CO)₄ produces nonclassical dihydrogen (and dinitrogen) complexes of the general form (η⁴-NBD)M(CO)₃(X₂) and (η²-NBD)M(CO)₄(X₂) (M = Cr, Mo, or W; X₂ = H₂, D₂, or N₂). These complexes have been identified by examination of their ν(C–O) IR spectra and comparison with complexes of similar structure. There are two isomers of a (NBD)M(CO)₃L complex, *fac* and *mer*. The M(CO)₃ moieties



in these complexes have different and highly characteristic ν(C–O) IR spectra [e.g., the recently isolated complexes²¹ *mer*- and *fac*-(NBD)M(CO)₃(olefin)]. The *mer* isomer has three bands, of which the highest frequency (the “in phase” symmetric stretch) is very weak and the other two, lower frequency, bands are often so close that they are not resolved. On the other hand, the *fac* isomer has three well-separated bands of comparable intensity. (NBD)M(CO)₃(H₂) (and N₂) complexes would be expected to have similar carbonyl spectra to (NBD)M(CO)₃(olefin) compounds because the bonding modes of η²-H₂ and of olefin ligands are closely related.^{6f}

(a) Primary Photoproducts: TRIR Spectroscopy of (NBD)M(CO)₄ (M = Cr, Mo, and W). The initial step in the photolysis of (NBD)M(CO)₄ at room temperature is clearly of considerable importance to the understanding of the overall hydrogenation process. One or more of the following processes might be expected to occur on flash photolysis of (NBD)M(CO)₄ in *n*-heptane solution: (a) dissociation of CO from an axial position, to yield axially solvated *fac*-(NBD)M(CO)₃(s) (s = *n*-heptane), (b) dissociation of CO from an equatorial position, to yield equatorially solvated *mer*-(NBD)M(CO)₃(s), (c) dechelation of the diene to give (η²-NBD)M(CO)₄(s). There are two possible isomers of this compound, with the solvent molecule coordinated either *cis* or *trans* to the η²-diene.



(19) Burdett, J. K.; Perutz, R. N.; Poliakov, M.; Turner, J. J. *Pure Appl. Chem.* **1977**, *49*, 271. Poliakov, M. *Inorg. Chem.* **1976**, *15*, 2892.

(20) Dobson, G. R.; Hodges, P. M.; Healy, M. A.; Poliakov, M.; Turner, J. J.; Firth, S.; Asali, K. J. *J. Am. Chem. Soc.* **1987**, *109*, 4218.

(21) Grevels, F.-W.; Jacke, J.; Betz, P.; Krueger, C.; Tsay, Y.-H. *Organometallics* **1989**, *8*, 293. Jacke, J. Doctoral Dissertation, University of Duisberg, F.R.G., 1989.

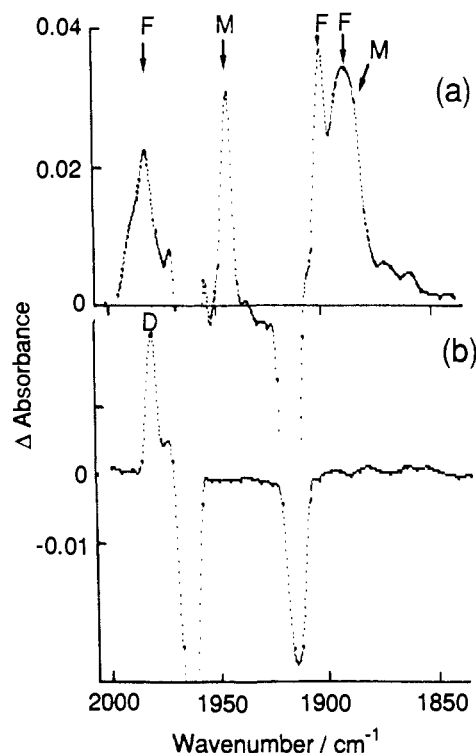


Figure 5. (a) TRIR spectrum corresponding to 5 μs after the flash photolysis of (NBD)Mo(CO)₄ in *n*-heptane under Ar (1 atm). Bands marked F and M are due to *fac*- and *mer*-(NBD)Mo(CO)₃(*n*-Hept), respectively. (b) TRIR spectrum corresponding to a delay of 1500 μs in the same reaction. The band D is due to an unidentified product formed by thermal reaction of the primary intermediates.²⁵ In both spectra, the negative peaks are due to (NBD)Mo(CO)₄ destroyed by the UV flash. These negative peaks have been somewhat truncated in spectrum (a).

Two separate sets of ν(C–O) bands are observed in the TRIR spectrum immediately after flash photolysis of (NBD)Mo(CO)₄ under an inert atmosphere of argon (Figure 5a). Two distinct photoproducts are formed on this time scale. One species, the shorter lived, has *three* ν(C–O) bands, marked F in Figure 5, while the other longer lived species has *two* ν(C–O) bands,^{22a} marked M. Both species appear to be primary photoproducts because the relative intensities of their bands in the TRIR spectrum remained unchanged when the power of the UV photolysis laser was halved. If one species were formed by secondary photolysis of the other, the relative intensities of the IR bands would be expected to change significantly when the UV power was reduced.

Both species were observed to decay faster under 1 atm pressure of CO (than under Ar) with complete regeneration of (NBD)Mo(CO)₄.^{22b} This indicates that both species are produced by loss of CO from (NBD)Mo(CO)₄, because fragments formed by dechelation of NBD [e.g. *cis*- or *trans*-(η²-NBD)Mo(CO)₄(s)] would react with CO to give (η²-NBD)Mo(CO)₅ rather than (NBD)Mo(CO)₄. (The IR bands of (η²-NBD)Mo(CO)₅ are known from TRIR experiments¹ with Mo(CO)₆ in the presence of NBD.)

(22) The lower frequency ν(C–O) band of the second species is not fully resolved from a band of the first species (see Figure 5a). However, kinetic measurements, described in our second paper,¹ clearly show that there are two distinct absorptions in this region, which decay with substantially different rates. The slower decay rate is very close to that of the absorption at 1944 cm⁻¹, suggesting that both bands belong to the same species. (b) The TRIR experiments under CO are made more difficult by the fact that there is a thermal reaction in the dark between (NBD)Mo(CO)₄ and CO which leads to the formation of Mo(CO)₆. Therefore, the solution of (NBD)Mo(CO)₄ was only pressurized with CO immediately before the start of the TRIR experiment. If the thermal formation of Mo(CO)₆ occurred during the course of the experiment, one would expect Mo(CO)₅ [ν(C–O) 1969 cm⁻¹] to be formed on flash photolysis. Measurements at 1969 cm⁻¹ were, therefore, made at frequent intervals throughout the experiment, and the solution was discarded as soon as significant amounts of Mo(CO)₅ were detected, typically after ca. 1 h.

Table III Wavenumbers of $\nu(\text{C-O})$ Bands (cm^{-1}) of the Primary Photoproducts in the Photolysis of $(\text{NBD})\text{M}(\text{CO})_4$ in Room Temperature *n*-Heptane Solution

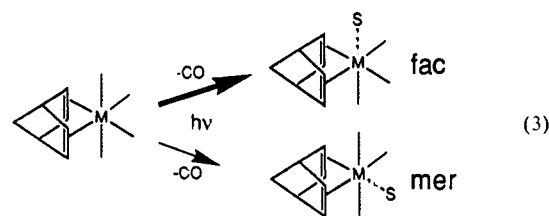
<i>fac</i> -(NBD)M(CO) ₃ (s)	TRIR ^a	matrix ^b
M = Cr	1978	1982.5
	1892	1894.7
	1888	1890.5
M = Mo	1988	1984.7
	1900	1899.0
	1893	1888.8
M = W	1981	1987.7
	1904	1903.9
	1890	1888.3
<i>mer</i> -(NBD)M(CO) ₃ (s)	TRIR ^a	matrix ^b
M = Cr	^c	2005.5
	1927	1928.8
	1884	1886.8
M = Mo	2016 ^{c,d}	2024
	1944	1950
	1884	(1900 ^e)
M = W	^c	
	1938	
	1884	

^a *s* = *n*-heptane. ^b Reference 23a, Ar matrix, 10 K. Data for *fac*-(NBD)Cr(CO)₃ and *mer*-(NBD)Mo(CO)₃ taken from ref 23b. ^c Band outside range of Nottingham TRIR spectrometer. ^d Band position measured at the Max Planck Institute für Strahlenchemie.²⁴ ^e Band position uncertain because of overlap.

Matrix isolation studies²³ on $(\text{NBD})\text{Mo}(\text{CO})_4$ have provided evidence for the formation of two primary photoproducts, *fac*-(η^4 -NBD)Mo(CO)₃ and *trans*-(η^2 -NBD)Mo(CO)₄, the yield of which is highly wavelength dependent, being favored by photolysis at 365 nm.²⁴ In the matrix, *mer*-(η^4 -NBD)Mo(CO)₃ is only observed as a secondary product^{23b} by photoisomerization of *fac*-(η^4 -NBD)Mo(CO)₃.

In our TRIR experiments at room temperature, the species with three $\nu(\text{C-O})$ bands can be identified as *fac*-(NBD)Mo(CO)₃(s) because of the similarity of its spectrum to that assigned to the analogous species in low temperature Ar matrices²³ (see Table III). The identification of the second species is rather more circumstantial; the TRIR experiments suggest that it is *mer*-(η^4 -NBD)Mo(CO)₃(s). The agreement with the matrix IR data is not quite as good as for the *fac* isomer, but there is uncertainty in the frequency of some of the matrix bands (see Table III). Furthermore, by comparison with the matrix^{23b} and LXe experiments (see below), one would not expect *mer*-(η^4 -NBD)Mo(CO)₃(s) to be a primary photoproduct. However, *mer*-(η^4 -NBD)Mo(CO)₃(s) appears to be the only obvious assignment, given that the species is a primary photoproduct, that its formation involves loss of CO, and that its reactions apparently lead to the formation of *mer*-(η^4 -NBD)Mo(CO)₃L species (see below). Thus, the TRIR experiments provide strong evidence that, at 308 nm, the primary photochemical pathway for $(\text{NBD})\text{Mo}(\text{CO})_4$ in room temperature solution is loss of CO (eq 3).

Loss of an axial CO group (with formation of *fac*-(NBD)-Mo(CO)₃(*n*-hept)) appears to be the major process in confirmation of Darensbourg and co-workers' elegant ¹³C tracer experiments.^{3b}



Although the TRIR data show that another photoproduct, most probably *mer*-(η^4 -NBD)Mo(CO)₃(*n*-hept) is also formed, there is no positive evidence for any process other than loss of CO. Nevertheless, dechelation of NBD apparently does occur in LXe (see below).

There is clearly a difference between the TRIR experiments, which strongly suggest that *mer*-(η^4 -NBD)Mo(CO)₃(*n*-hept) is formed as a primary photoproduct (albeit a minor one), and matrix²³ and LXe experiments, which do not. This difference may be a wavelength effect but more probably reflects the difference in temperature between the two sets of experiments. However, the results described in our second paper¹ suggest that this difference in photoproducts is not crucial to the overall mechanism of catalytic hydrogenation.

In the absence of added CO, the bands of *fac*- and *mer*-(NBD)Mo(CO)₃(s) decay until, after 1500 μs , the TRIR spectrum contains only a single new band,²⁵ marked "D" in Figure 5b. A similar $\nu(\text{C-O})$ band is also observed when $(\text{NBD})\text{Mo}(\text{CO})_4$ is photolysed in LXe without added ligands (e.g., N₂, etc.), and it is stable in LXe for at least 1 h at -90 °C (see below). Our TRIR kinetic measurements¹ show that, under catalytic conditions at room temperature, formation of "D" would be a very minor process compared to the reaction of the intermediates with either NBD or H₂. Thus it is improbable that this species plays a significant role in the overall hydrogenation cycle.

Less detailed TRIR experiments were performed on $(\text{NBD})\text{M}(\text{CO})_4$ (M = Cr and W). The IR data are summarized in Table III and quantitative kinetic measurements (for W) are in our second paper.¹ The experiments show that the photochemistry of W is broadly similar to that of Mo. For Cr, intermediates are very much more reactive than their Mo or W analogues. Both *fac*- and *mer*-(NBD)Cr(CO)₃(s) appear to be formed, but given the short lifetimes of the intermediates, the spectra are only assigned by comparison with the matrix data.²³ However, the agreement between the TRIR and matrix spectra are striking. We now consider the reactions of these $(\text{NBD})\text{M}(\text{CO})_3$ (s) intermediates with N₂ and H₂.

(b) Photochemical Reaction of $(\text{NBD})\text{M}(\text{CO})_4$ with N₂. When $(\text{NBD})\text{Mo}(\text{CO})_4$ is flash photolysed in *n*-heptane under 1 atm pressure of N₂, the TRIR spectrum reveals the formation of the same primary photoproducts, *fac*- and *mer*-(NBD)M(CO)₃(s), as were observed under Ar. The initial TRIR spectrum (not illustrated) is the same as that in Figure 5a. However, the TRIR spectrum, corresponding to 1500 μs after the UV flash (Figure 6a), is quite different from that under Ar (Figure 5b). Apart from the band due to species D, there are four new bands, assignable to two different dinitrogen complexes. The TRIR kinetics¹ show that one complex has three $\nu(\text{C-O})$ bands (marked with asterisks in Figure 6a) and is formed from *fac*-(NBD)Mo(CO)₃(s). The other product has a single $\nu(\text{C-O})$ band (arrowed) in this wavenumber region and is formed from the second intermediate. The spectra of the two products are similar to those of the *fac*- and *mer*-(NBD)M(CO)₃(olefin) complexes.²¹ Thus the products are reasonably identified²⁶ as *fac*- and *mer*-(NBD)Mo(CO)₃(N₂),

(23) (a) Hooker, R. H.; Rest, A. J. *XIth Int. Conf. Organomet. Chem.* Abstr. 36. Hooker, R. H. Ph.D. Thesis, University of Southampton, U.K., 1987. (b) Grevels, F.-W.; Jacke, J.; Klotzbücher, W. E.; Schaffner, K.; Hooker, R. H.; Rest, A. J. *J. Organomet. Chem.*, in press.

(24) Our TRIR experiments were all carried out with 308-nm photolysis (dictated by the XeCl laser), and we have not detected the $\nu(\text{C-O})$ band of *trans*-(η^2 -NBD)M(CO)₄(s) in solution at room temperature. Exactly the same spectra were obtained with the TRIR spectrometer in Mülheim which is based on an IR globar rather than a tunable CO laser (for example, see: Hermann, H.; Grevels, F.-W.; Henne, A.; Schaffner, K. *J. Phys. Chem.* 1982, 86, 5151. Church, S. P.; Grevels, F.-W.; Hermann, H.; Schaffner, K. *Inorg. Chem.* 1985, 24, 418). The globar gives the apparatus a wider wavenumber range than that of a Nottingham, and this enabled us to detect the "missing" $\nu(\text{C-O})$ band of *mer*-(NBD)Mo(CO)₃ at 2016 cm^{-1} .

(25) Although $(\text{NBD})\text{Mo}(\text{CO})_4$ is known to form Mo(CO)₆ in the course of prolonged UV photolysis, D is not Mo(CO)₆, which absorbs at a higher frequency. There may, of course, be other bands of D masked by those of $(\text{NBD})\text{Mo}(\text{CO})_4$, but, given only one $\nu(\text{C-O})$ band, we cannot draw any conclusions about the structure of D from the spectrum in Figure 5b. TRIR measurements at Mülheim indicate that D has a lifetime of 0.1–0.2 s. It is possible that D is a dinuclear species formed by reaction of the intermediates with unphotolysed $(\text{NBD})\text{Mo}(\text{CO})_4$, particularly because the formation of such species has been found to be quite widespread in other systems (e.g. ref 20).

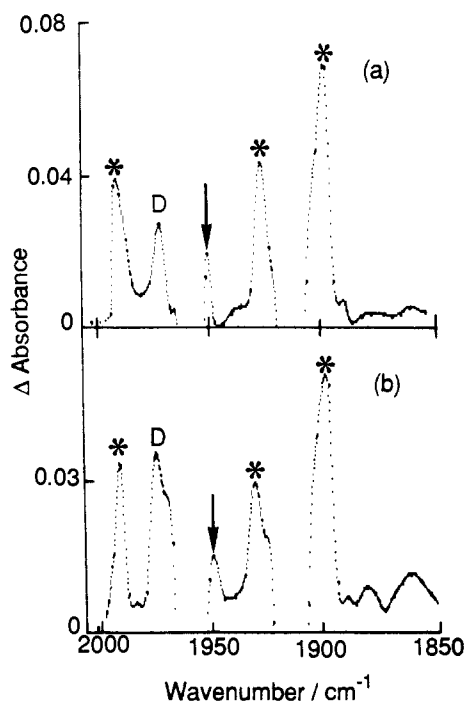


Figure 6. TRIR spectra corresponding to 1500 μ s after the flash photolysis of $(\text{NBD})\text{Mo}(\text{CO})_4$ under 1 atm pressure: (a) dinitrogen and (b) dihydrogen. Bands marked with an asterisk are due to *fac*- $(\text{NBD})\text{Mo}(\text{CO})_3(\text{X}_2)$ ($\text{X}_2 = \text{N}_2$ or H_2 , respectively), and the arrowed band is assigned to the *mer* isomer. In both spectra the band D is due to a secondary product²⁵ which does not involve either N_2 or H_2 (see Figure 5). Note that in both TRIR spectra the negative peaks due to the parent $(\text{NBD})\text{M}(\text{CO})_4$ destroyed by the UV flash have been omitted to make comparison between the two spectra easier.

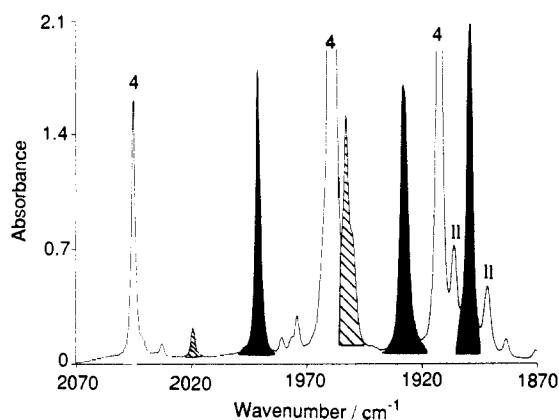


Figure 7. IR spectra in the $\nu(\text{C}-\text{O})$ region showing the products generated after 5 min of UV photolysis of a solution of $(\text{NBD})\text{Mo}(\text{CO})_4$ in LXe doped with N_2 (150 psi) at -90°C . The bands labeled 4 are due to unreacted $(\text{NBD})\text{Mo}(\text{CO})_4$, and the other bands, assigned to products, are marked as follows: black, *fac*- $(\text{NBD})\text{Mo}(\text{CO})_3(\text{N}_2)$; cross-hatched, *mer*- $(\text{NBD})\text{Mo}(\text{CO})_3(\text{N}_2)$; II, disubstituted secondary photoproduct $(\text{NBD})\text{Mo}(\text{CO})_2(\text{N}_2)_2$.

an assignment which is supported by experiments in LXe.

The broad-band UV photolysis of $(\text{NBD})\text{Mo}(\text{CO})_4$ in LXe doped with N_2 generates several species, in particular one with three $\nu(\text{C}-\text{O})$ bands and another with two (Figure 7). The wavenumbers of the $\nu(\text{C}-\text{O})$ bands (Table IV) are in very close agreement with those observed in the TRIR experiment with $(\text{NBD})\text{Mo}(\text{CO})_4$ in *n*-heptane saturated with N_2 at room tem-

(26) The identification of *mer*- $(\text{NBD})\text{Mo}(\text{CO})_3(\text{N}_2)$ from one weak band in the TRIR spectra is clearly more tentative than the identification of the *fac* isomer, which has three relatively strong bands. However, the low intensity of the band assigned to *mer*- $(\text{NBD})\text{Mo}(\text{CO})_3(\text{N}_2)$ is due, at least in part, to overlap with the strong negative peak due to the parent $(\text{NBD})\text{M}(\text{CO})_4$ destroyed by the UV flash.

Table IV. Wavenumbers of the $\nu(\text{C}-\text{O})$ IR Bands (cm^{-1}), of Photoproducts of $(\text{NBD})\text{Mo}(\text{CO})_4$ with N_2 and H_2 under Various Conditions

	TRIR ^a	Matrix ^b	LXe ^c	
<i>fac</i> - $(\text{NBD})\text{Mo}(\text{CO})_3(\text{N}_2)$	<i>d</i>	2231	2219.6	$\nu(\text{N}-\text{N})$
	1994	1990.5	1991	<i>a'</i>
	1930	1926.2	1928	<i>a''</i>
<i>mer</i> - $(\text{NBD})\text{Mo}(\text{CO})_3(\text{N}_2)$	<i>d</i>	1900	1896.4	<i>a''</i>
	<i>d</i>	<i>e</i>	2163.3	$\nu(\text{N}-\text{N})$
	1956		2019	<i>a'</i>
$(\text{NBD})\text{Mo}(\text{CO})_2(\text{N}_2)_2$			1950	<i>a' + a''</i>
			2144.5	$\nu(\text{N}-\text{N})$
	<i>e</i>	<i>e</i>	1906.3	
$(\eta^2\text{-NBD})\text{Mo}(\text{CO})_4(\text{N}_2)^f$	<i>d</i>	2195	2187.6	$\nu(\text{N}-\text{N})$
	<i>e</i>		1891.8	
			1928	
<i>fac</i> - $(\text{NBD})\text{Mo}(\text{CO})_3(\text{H}_2)$	1998		1997.0	<i>a'</i>
	1930	<i>e</i>	1930.0	<i>a''</i>
	1900		1898.3	<i>a'</i>
<i>mer</i> - $(\text{NBD})\text{Mo}(\text{CO})_3(\text{H}_2)$	<i>d</i>		2029.3	<i>a'</i>
	1952		1952	<i>a' + a''</i>
			2060	
$(\eta^2\text{-NBD})\text{Mo}(\text{CO})_4(\text{H}_2)$			1964	
			1941.3	

^aThis work, *n*-heptane solution, 25°C . ^bReference 23a, nitrogen matrix, 10 K (similar results have been obtained^{23b}). ^cLiquid xenon solution, -90°C . Data refers to D_2 rather than H_2 derivatives. ^dNot observed. This band is expected to lie outside the range of the TRIR spectrometer. ^eNot reported. ^fSee ref 31.

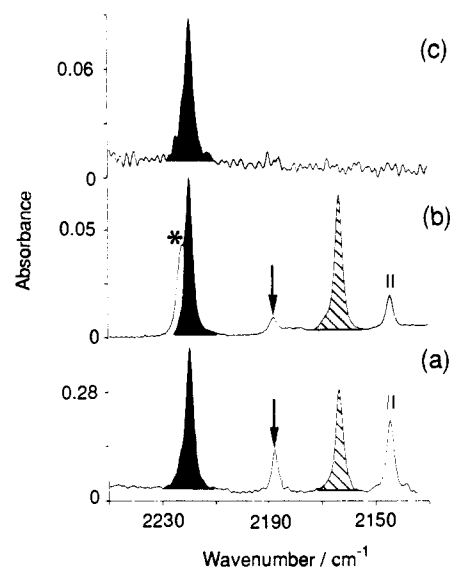


Figure 8. IR spectra in the $\nu(\text{N}-\text{N})$ region illustrating bands due to dinitrogen complexes formed in LXe doped with N_2 (a) by 5 min of UV photolysis of $(\text{NBD})\text{Mo}(\text{CO})_4$, (b) by 15 min of UV photolysis of *mer*- $(\text{NBD})\text{Mo}(\text{CO})_3(\text{C}_2\text{H}_4)$, and (c) by thermal reaction with N_2 of the photoproducts of $(\text{NBD})\text{Mo}(\text{CO})_4 + \text{D}_2$ [i.e., $(\text{NBD})\text{Mo}(\text{CO})_4$ was photolysed in LXe doped with D_2 , the D_2 was then vented, and a pressure of N_2 was added to the solution]. The bands are assigned as follows: black, *fac*- $(\text{NBD})\text{Mo}(\text{CO})_3(\text{N}_2)$; arrowed $(\eta^2\text{-NBD})\text{Mo}(\text{CO})_4(\text{N}_2)$;³¹ cross-hatched, *mer*- $(\text{NBD})\text{Mo}(\text{CO})_3(\text{N}_2)$; II, disubstituted secondary photoproduct³⁰ $(\text{NBD})\text{Mo}(\text{CO})_2(\text{N}_2)_2$ (the band marked with an asterisk, in spectrum (b), is tentatively assigned to $(\text{NBD})\text{Mo}(\text{CO})_2(\text{C}_2\text{H}_4)(\text{N}_2)$). Note that there is no obvious absorption due to free CO liberated by the photolysis because, under these conditions, the band of CO is extremely broad and weak by comparison with the $\nu(\text{N}-\text{N})$ absorptions.

perature (Figure 6a). In LXe, a single $\nu(\text{N}-\text{N})$ band is observed for each photoproduct, clearly indicating the presence of coordinated N_2 in both species (Figure 8a). Exactly the same N_2 species²⁷ were observed when *mer*- $(\text{NBD})\text{Mo}(\text{CO})_3(\text{C}_2\text{H}_4)$ was

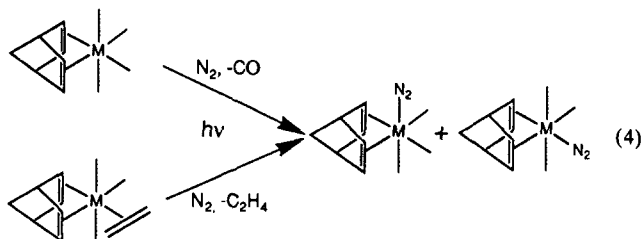
(27) In addition, there is a relatively minor $\nu(\text{N}-\text{N})$ absorption (a shoulder at 2223 cm^{-1} , marked with an asterisk in Figure 8b). This shoulder is not observed during the photolysis of $(\text{NBD})\text{Mo}(\text{CO})_4$ and presumably arises by loss of CO from the ethene complex.

Table V. IR Wavenumbers (cm^{-1}) in the $\nu(\text{C-O})$ and $\nu(\text{N-N})$ Region of the N_2 and D_2 Photoproducts of $(\text{NBD})\text{M}(\text{CO})_4$ Complexes in Liquid Xe^a

	Cr	Mo	W	assignment
$(\text{NBD})\text{M}(\text{CO})_4$	2030.2	2044.0	2042.0	a_1
	1955.7	1959.4	1956.0	a_1
	1944.2	1959.0	1956.0	b_1
	1913.2	1914.2	1909.2	b_2
<i>fac</i> - $(\text{NBD})\text{M}(\text{CO})_3(\text{N}_2)$	2198.9	2219.6	2200.9	$\nu(\text{N-N})$ a'
	1987.3	1991.3	1992.3	a'
	1921.9	1927.8	1932.1	a''
	1900.6	1899.2	1896.9	a'
<i>mer</i> - $(\text{NBD})\text{M}(\text{CO})_3(\text{N}_2)$	2172.4	2163.3	2169.2	$\nu(\text{N-N})$ a'
	2002.7	2019.6	2016.5	a'
	1937.2	1953.1		c
		1951 sh		a''
$(\text{NBD})\text{M}(\text{CO})_2(\text{N}_2)_2$	2147.8	2144.5	2133	$\nu(\text{N-N})$
	1910.6	1906.3	1908.3	
	1895.5	1891.8	c	
<i>fac</i> - $(\text{NBD})\text{M}(\text{CO})_3(\text{D}_2)$	1991.8	1997.0	1997.7	a'
	1923.7	1930.0	1931.7	a''
	1897.7	1898.3	1888.7	a'
				$a' + a''$
<i>mer</i> - $(\text{NBD})\text{M}(\text{CO})_3(\text{D}_2)$	2012.9	2029.3	b	a'
	1936.1	1941.3		$a' + a''$
$(\eta^2\text{-NBD})\text{M}(\text{CO})_4(\text{D}_2)$		2060	2062.7	
		1964	1967.0 ^d	
		1941.3	1944.6 ^d	

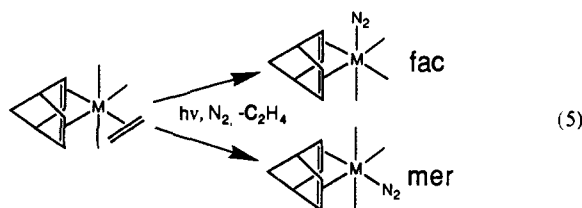
^a Value in LXe at -91°C . ^b Not observed. ^c Obscured by stronger bands in solution. ^d Bands shift to 1967.6 and 1947.2 cm^{-1} when the experiment is repeated with H_2 .

photolysed in LXe doped with N_2 (Figure 8b). In addition, bands due to uncoordinated C_2H_4 could be observed after the photolysis (1437 and 943 cm^{-1}).²⁸ The two photoproducts must both contain the $(\text{NBD})\text{Mo}(\text{CO})_3$ moiety since they can be generated from either $(\text{NBD})\text{Mo}(\text{CO})_4$ or *mer*- $(\text{NBD})\text{Mo}(\text{CO})_3(\text{C}_2\text{H}_4)$. The positions and relative intensities of the $\nu(\text{C-O})$ bands²⁹ identify these photoproducts as *fac*- and *mer*- $(\text{NBD})\text{Mo}(\text{CO})_3(\text{N}_2)$, both of which are stable at -90°C in LXe as summarized in eq 4.



There is close agreement between the IR spectra observed in LXe doped with N_2 (Figure 7) and with those reported²³ for similar experiments in solid N_2 matrices at 10 K. IR data for TRIR, LXe, and some of the matrix experiments are summarized in Table IV. However, when the spectra in LXe are examined in more detail, significant differences from the TRIR experiment begin to emerge. Two additional bands are observed in the $\nu(\text{N-N})$ region (Figure 8). One band, marked II, is only observed after prolonged photolysis of either $(\text{NBD})\text{Mo}(\text{CO})_4$ or *mer*- $(\text{NBD})\text{Mo}(\text{CO})_3(\text{C}_2\text{H}_4)$ and is clearly due to a secondary photolysis product,³⁰ probably $(\text{NBD})\text{Mo}(\text{CO})_2(\text{N}_2)_2$. The second $\nu(\text{N-N})$

band, arrowed in Figure 8a, is due to a species formed *directly* from $(\text{NBD})\text{Mo}(\text{CO})_4$, because it is detectable even after only a few seconds of photolysis. However, unlike the other $\nu(\text{N-N})$ bands, the intensity of this band rapidly reaches a constant value so that, after prolonged photolysis, it appears relatively weak. No corresponding $\nu(\text{C-O})$ bands can be identified, presumably because of overlap with stronger bands in this rather congested region of the spectrum. By contrast, this $\nu(\text{N-N})$ band is only observed after more prolonged photolysis of *mer*- $(\text{NBD})\text{Mo}(\text{CO})_3(\text{C}_2\text{H}_4)$ (Figure 8b). This evidence suggests that the band is due to $(\eta^2\text{-NBD})\text{Mo}(\text{CO})_4(\text{N}_2)$, which could be formed directly from $(\text{NBD})\text{Mo}(\text{CO})_4$ but not from $(\text{NBD})\text{Mo}(\text{CO})_3(\text{C}_2\text{H}_4)$. In addition, the $\nu(\text{N-N})$ band correlates well, allowing for a small solvent shift, with one tentatively assigned to $(\eta^2\text{-NBD})\text{Mo}(\text{CO})_4(\text{N}_2)$ in matrix isolation experiments^{23,31} (Table IV). There is a further difference between the photolysis of $(\text{NBD})\text{Mo}(\text{CO})_4$ and $(\text{NBD})\text{Mo}(\text{CO})_3(\text{C}_2\text{H}_4)$ under these conditions; *mer*- $(\text{NBD})\text{Mo}(\text{CO})_3(\text{N}_2)$ appears to be formed by photolysis of the ethene complex (eq 5) but not of $(\text{NBD})\text{Mo}(\text{CO})_4$, where the



principal route to *mer*- $(\text{NBD})\text{Mo}(\text{CO})_3(\text{N}_2)$ appears to be through secondary photolysis.³² This result is consistent with Darensbourg's observation³ of predominant substitution of the axial CO group in $(\text{NBD})\text{Mo}(\text{CO})_4$.

The formation of *fac*- $(\text{NBD})\text{Mo}(\text{CO})_3(\text{N}_2)$ by photolysis of *mer*- $(\text{NBD})\text{Mo}(\text{CO})_3(\text{C}_2\text{H}_4)$ clearly involves isomerization of the $(\text{NBD})\text{Mo}(\text{CO})_3$ moiety. This isomerization is reminiscent of the formation of *cis*- $\text{M}(\text{CO})_4(\text{C}_2\text{H}_4)(\text{N}_2)$ from *trans*- $\text{M}(\text{CO})_4(\text{C}_2\text{H}_4)_2$, which we described above. In our second paper,¹ we suggest that the analogous isomerization of $(\eta^4\text{-NBD})(\eta^2\text{-NBD})\text{M}(\text{CO})_3$ species is an important step in the overall cycle for the catalytic hydrogenation of NBD. When $(\text{NBD})\text{Cr}(\text{CO})_4$ ³³ or $(\text{NBD})\text{W}(\text{CO})_4$ ³⁴ is photolysed in LXe doped with N_2 , the products *fac*- and *mer*- $(\text{NBD})\text{M}(\text{CO})_3(\text{N}_2)$ can be identified. In both cases, a disubstituted product $(\text{NBD})\text{M}(\text{CO})_2(\text{N}_2)_2$ is also generated. There is, however, a difference between the two metals; $(\eta^2\text{-NBD})\text{W}(\text{CO})_4(\text{N}_2)$ is observed under these conditions while the Cr analogue is not. All of the N_2 products are stable in LXe under a pressure of 150 psi N_2 , for at least 1 hr at -91°C . The IR bands of all these N_2 species are included in Table V.

The differences which we have observed between the LXe and TRIR experiments can probably be attributed to differences in temperature and photolysis sources (broad-band Hg arc vs narrow-band XeCl laser) and serve to underline the considerable wavelength dependence of the photochemistry of these compounds. Clearly, however, the experiments are complementary; the higher resolution and wider wavenumber range of the IR data in the LXe experiments strengthen and confirm the assignments of the TRIR spectra.

(c) **Photochemical Reaction of $(\text{NBD})\text{M}(\text{CO})_4$ with H_2 and D_2 .** The TRIR spectrum corresponding to 1500 μs after the flash

(28) Duckett, S. B.; Haddleton, D. M.; Jackson, S. A.; Perutz, R. N.; Poliakov, M.; Upmacis, R. K. *Organometallics* **1988**, *7*, 1526.

(29) Furthermore, the relative frequencies of the $\nu(\text{N-N})$ bands (*fac* > *mer*) is consistent with Darensbourg's observation³ that the energy factored force constant, $k_{\text{C-O}}$, of an axial CO group in $(\text{NBD})\text{Mo}(\text{CO})_4$ is higher than that of an equatorial group in the parent molecule, $(\text{NBD})\text{Mo}(\text{CO})_4$.

(30) New bands can also be seen in the $\nu(\text{C-O})$ region (1906.3 and 1891.8 cm^{-1}), but there is some overlap with the bands of other species in solution (see Figure 7). These two bands are consistent with the secondary product being $(\text{NBD})\text{Mo}(\text{CO})_2(\text{N}_2)_2$, but there is insufficient information to assign the bands conclusively to one of the three possible isomers of this complex. This secondary photoproduct was not observed in the TRIR experiments because they arise from photolysis of $(\text{NBD})\text{Mo}(\text{CO})_3(\text{N}_2)$ species which are formed a relatively long time after the UV laser flash. The laser pulse has a duration of 20 ns, while the N_2 products are produced¹ over a period of more than 50 μs .

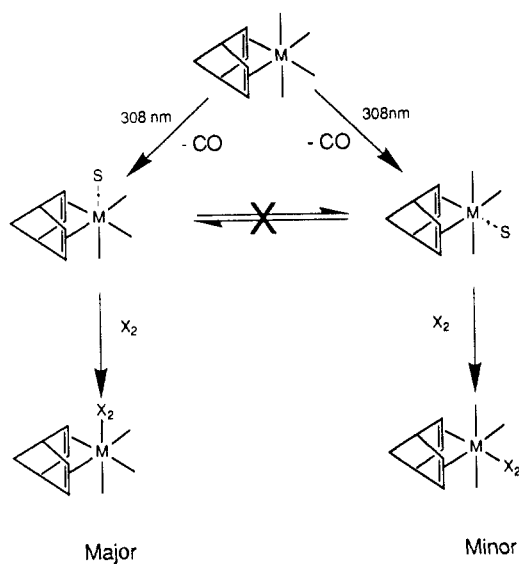
(31) Rest^{23a} originally assigned this band to *cis*- $(\eta^2\text{-NBD})\text{Mo}(\text{CO})_4(\text{N}_2)$, but both matrix studies²⁵ suggest that the $\nu(\text{C-O})$ bands of this species would be masked in our LXe experiment. We, however, cannot distinguish between the *cis* and *trans* isomers of $(\eta^2\text{-NBD})\text{Mo}(\text{CO})_4(\text{N}_2)$ in our LXe experiment, since we have not been able to assign $\nu(\text{C-O})$ bands to this compound. However, this problem does not arise in our experiments³⁸ with D_2 .

(32) We have found similar results for formation of $(\text{NBD})\text{Mo}(\text{CO})_3(\text{C}_2\text{H}_4)$ in LXe where the *fac* isomer is formed before the *mer*.¹

(33) Our results for $(\text{NBD})\text{Cr}(\text{CO})_4$ in LXe are in general agreement with those obtained by Andrea and co-workers (Oskam, A.; Andrea, R. R.; Stufkens, D. J.; Vuurman, M. A. Royal Soc. Chem. Congress, Swansea, 1987; Poster D10. Andrea, R. R. Ph.D. Thesis, University of Amsterdam, 1989).

(34) The sample of $(\text{NBD})\text{W}(\text{CO})_4$ contained a trace of $\text{W}(\text{CO})_6$ which was present in the solution at the start of the experiment. Therefore, bands due to $\text{W}(\text{CO})_5(\text{N}_2)$ were also observed after UV photolysis.

Scheme III



photolysis of $(\text{NBD})\text{Mo}(\text{CO})_4$ in *n*-heptane under 1 atm pressure of H_2 is shown in Figure 6b. The spectrum is similar to³⁵ but not identical with that observed under N_2 (Figure 6a), indicating that the photoproducts have the same basic structure. As with N_2 , the kinetics indicate that there are two products, one formed from *fac*- $(\text{NBD})\text{Mo}(\text{CO})_3(\text{s})$ and the other formed from the second intermediate, probably *mer*- $(\text{NBD})\text{Mo}(\text{CO})_3(\text{s})$ (Scheme III).

Thus, the product bands are assigned to the nonclassical complexes *fac*- and *mer*- $(\text{NBD})\text{Mo}(\text{CO})_3(\text{H}_2)$ by comparison with the spectra of the N_2 analogues. Less detailed studies with $(\text{NBD})\text{Cr}(\text{CO})_4$ and $(\text{NBD})\text{W}(\text{CO})_4$ suggest that the corresponding $\eta^2\text{-H}_2$ compounds are formed. These results are strongly supported by experiments in LXe solution.

Figure 9a shows the $\nu(\text{C-O})$ region of the IR spectrum obtained after the photolysis of $(\text{NBD})\text{Mo}(\text{CO})_4$ dissolved in LXe doped with D_2 . The characteristic band patterns of *fac*- and *mer*- $(\text{NBD})\text{M}(\text{CO})_3(\text{L})$ compounds can easily be recognized in Figure 9a. These bands are close in wavenumber to those observed in the TRIR experiment and also to the bands of the corresponding N_2 products in LXe. The bands are not observed when the compound is photolysed in the absence of D_2 . Bands due to these same species³⁶ are also generated by photolysis of *mer*- $(\text{NBD})\text{Mo}(\text{CO})_3(\text{C}_2\text{H}_4)$, although one *mer* band is obscured by the absorption of the unreacted ethene complex (Figure 9b). All of these results support the assignment of these bands to the nonclassical complexes, *fac*- and *mer*- $(\text{NBD})\text{Mo}(\text{CO})_3(\text{D}_2)$. As already found with the N_2 complexes, the *mer* isomer is not generated from $(\text{NBD})\text{Mo}(\text{CO})_4$ as rapidly as the *fac*, indicating that the principal route to the *mer* isomer is via secondary photolysis, presumably of the *fac* isomer.

In addition to the *fac* and *mer* bands, there are three $\nu(\text{C-O})$ bands (arrowed in Figure 9a) due to a species, X, generated directly from $(\text{NBD})\text{Mo}(\text{CO})_4$, which is not observed in the absence of D_2 (or H_2). X is not generated when *mer*- $(\text{NBD})\text{Mo}(\text{CO})_3(\text{C}_2\text{H}_4)$ is photolysed in the presence of D_2 (Figure 9b). Thus, we can eliminate the possibility that X is a classical dihydride in thermal equilibrium with the nonclassical $(\text{NBD})\text{Mo}(\text{CO})_3(\text{D}_2)$ species.³⁷ We have already shown that $(\eta^2\text{-}$

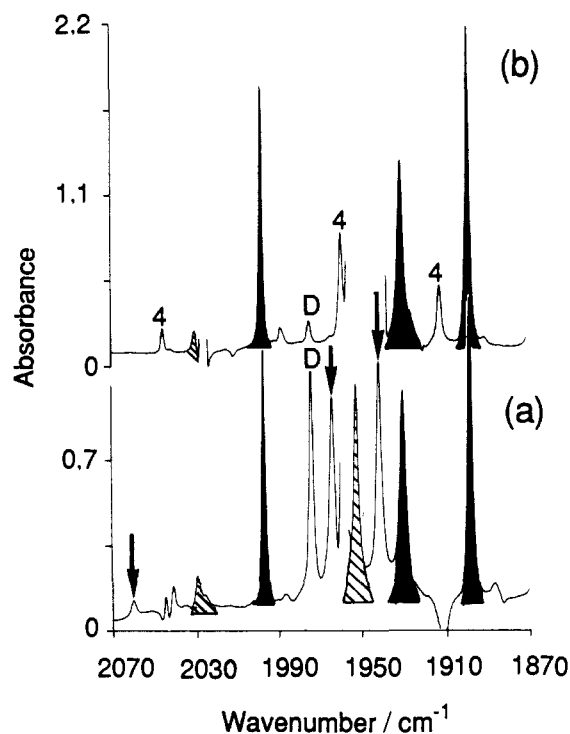
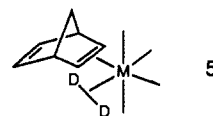


Figure 9. IR spectra showing bands in the $\nu(\text{C-O})$ region due to the photoproducts generated in LXe doped with D_2 (150 psi) at -90°C by (a) 25 min of UV photolysis of $(\text{NBD})\text{Mo}(\text{CO})_4$ and (b) 15 min of UV photolysis of *mer*- $(\text{NBD})\text{Mo}(\text{CO})_3(\text{C}_2\text{H}_4)$. In both spectra, the bands due to the starting compounds have been removed by computer subtraction (the bands labeled 4 in spectrum (b) are due to a trace impurity of $(\text{NBD})\text{Mo}(\text{CO})_4$ in the starting material). The products are marked as follows: black, *fac*- $(\text{NBD})\text{Mo}(\text{CO})_3(\text{D}_2)$; cross-hatched, *mer*- $(\text{NBD})\text{Mo}(\text{CO})_3(\text{D}_2)$; arrowed, $(\eta^2\text{-NBD})\text{Mo}(\text{CO})_4(\text{D}_2)$, which is only generated from $(\text{NBD})\text{Mo}(\text{CO})_4$; (the band labeled D is due to an unidentified product²⁵ that is formed slowly even when $(\text{NBD})\text{Mo}(\text{CO})_4$ is photolysed in LXe in the absence of D_2).

$(\text{NBD})\text{Mo}(\text{CO})_4(\text{N}_2)$ can be generated under similar photolytic conditions in the presence of N_2 and the IR bands of the NBD photoproduct are similar in wavenumber to those of $(\text{C}_2\text{H}_4)\text{Mo}(\text{CO})_4(\text{D}_2)$ (Table II). We therefore assign these bands to a $(\eta^2\text{-NBD})\text{Mo}(\text{CO})_4(\text{D}_2)$ complex, 5, most probably the *cis* isomer.³⁸



(37) During the subsequent thermal reactions and decay of these species, the bands of *fac*- $(\text{NBD})\text{Mo}(\text{CO})_3(\text{D}_2)$ decay much faster than those arrowed. Similarly, the bands of *mer*- $(\text{NBD})\text{Mo}(\text{CO})_3(\text{D}_2)$ grow in during photolysis significantly slower than the X bands. These observations provide further evidence against any thermal equilibrium existing between these species.

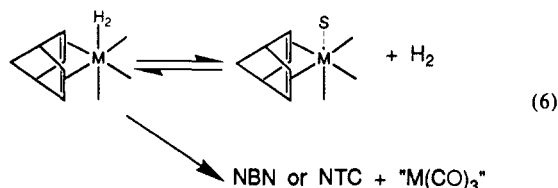
(38) Photolysis of $(\text{NBD})\text{Mo}(\text{CO})_4$ in pure CO matrices²³ generates what is presumed to be $(\eta^2\text{-NBD})\text{Mo}(\text{CO})_5$. Although the bands of this species [$\nu(\text{C-O})$ 2079, 1966, and 1941 cm^{-1}] are similar to those of our D_2 product, it is unlikely that $(\eta^2\text{-NBD})\text{Mo}(\text{CO})_5$ would be generated in our LXe experiment. One cannot use spectroscopic arguments to eliminate the possibility that the bands are due to $(\eta^2\text{-NBN})\text{Mo}(\text{CO})_4(\text{D}_2)$, formed by hydrogenation of NBD. However, this assignment is unlikely because there is no reason why this NBN compound should be formed by photolysis of $(\text{NBD})\text{Mo}(\text{CO})_4$ but not a *mer*- $(\text{NBD})\text{Mo}(\text{CO})_3(\text{C}_2\text{H}_4)$. Thus $(\eta^2\text{-NBD})\text{Mo}(\text{CO})_4(\text{D}_2)$ is the most probable assignment. Four $\nu(\text{C-O})$ bands ($3a' + a''$) are predicted for the *cis* isomer of $(\eta^2\text{-NBD})\text{Mo}(\text{CO})_4(\text{D}_2)$ and either two ($a_1 + e$) or three ($a_1 + b_1 + b_2$) for the *trans* isomer depending on whether the $\eta^2\text{-NBD}$ ligand reduces the local symmetry of the $\text{M}(\text{CO})_4$ moiety from C_4 to C_{2v} . Three $\nu(\text{C-O})$ bands are observed (see Table V). The separation of the two lower frequency bands ca. 21 cm^{-1} is rather larger than had previously been observed for the splitting of an *e* mode by an $\eta^2\text{-alkene}$ ¹³ so we favor the assignment to the *cis* isomer. However, this assignment is in contrast to the reaction of matrix isolated $(\text{NBD})\text{Mo}(\text{CO})_4$ with N_2 which appears^{23b} to lead to *trans*- $(\eta^2\text{-NBD})\text{Mo}(\text{CO})_4(\text{N}_2)$.

(35) The band D is somewhat stronger in Figure 6b (under H_2) than in Figure 6a (under N_2). This is consistent with the solubility of H_2 , which is lower than that of N_2 in organic solvents.¹

(36) Small amounts of *fac*- $(\text{NBD})\text{Mo}(\text{CO})_3$ and $(\text{NBD})\text{Mo}(\text{CO})_4$ are also formed during photolysis, but the main products indicate that the preferred reaction is the photosubstitution of ethene by D_2 . In this experiment, a very weak and broad absorption was observed at 2250 cm^{-1} with a corresponding band at ca. 3080 cm^{-1} when the experiment was repeated with H_2 . These bands may well be the $\nu(\text{D-D})$ and $\nu(\text{H-H})$ bands of the nonclassical dihydrogen groups, but, given their low intensity, they could also be overtones or combination bands.

The Cr complexes, *fac*- and *mer*-(NBD)Cr(CO)₃(D₂), can be generated by photolysis of (NBD)Cr(CO)₄ in LXe doped with D₂, although they are thermally very much less stable than their N₂ analogues (see Table V). The difference in the thermal stabilities of the D₂ and N₂ products is striking; the D₂ products seem to be much less stable than might be expected from the relative stabilities of the analogous ethene/D₂ adducts (see above). As with the N₂ experiments (above), there is no evidence for the formation of an η^2 -NBD/Cr complex. When (NBD)W(CO)₄ was photolyzed in LXe doped with D₂, the principal product had ν (C–O) bands, similar in wavenumber to those assigned to (η^2 -NBD)Mo(CO)₄(D₂) in the photolysis of (NBD)Mo(CO)₄ (see above). These bands were slightly shifted when H₂ was used instead of D₂, and we, therefore, identify this product as (η^2 -NBD)W(CO)₄(D₂). Unlike Cr or Mo, there were no bands which could be assigned to *mer*-(NBD)W(CO)₃(D₂) in our LXe experiments. This could be an effect of the photolysis wavelength (the W system appears to be wavelength dependent¹ at room temperature but not in a matrix^{23b}). Alternatively, it may merely reflect the thermal instability of the *mer*-(NBD)W(CO)₃(D₂), because the corresponding H₂ species was detected in our fast TRIR experiments at room temperature.

(d) **Thermal Reactions of Nonclassical Dihydrogen Species.** The nonclassical complexes described in the previous section have two possible modes of decay: (i) dissociative loss of the η^2 -H₂ group or (ii) hydrogenation of the NBD to form NBN or NTC (eq 6).



In principle, one can distinguish between these pathways by comparing the rate of decay under different pressures of H₂. If dissociative loss of H₂ were occurring, an increase in hydrogen pressure should increase the lifetime of the η^2 -H₂ compound.^{16,40} If, however, the hydrogen compound were to decay by hydrogenation of the NBD, the rate of this intramolecular reaction (and therefore the lifetime of the η^2 -H₂ compound) should be unaffected by changes in the hydrogen pressure. Figure 10b shows TRIR kinetic traces corresponding to the decay of *fac*(NBD)Mo(CO)₃(H₂) in *n*-heptane at room temperature.⁴¹ The lifetime of this compound is clearly prolonged by a higher pressure of hydrogen, suggesting that it decays by dissociative loss of H₂ rather than by hydrogenation of NBD. The opposite result was found for the decay of *fac*-(NBD)Cr(CO)₃(D₂) (Figure 10a) where the lifetime was unaltered by increasing the pressure of H₂. Below, we propose that this difference in behavior reflects the difference in catalytic behavior of the two metals. Similarly, the decay of *mer*-(NBD)Cr(CO)₃(H₂) did not depend on hydrogen concentration not only in *n*-heptane at room temperature but also in LXe. *mer*-(NBD)Cr(CO)₃(H₂) was allowed to decay in LXe under 160

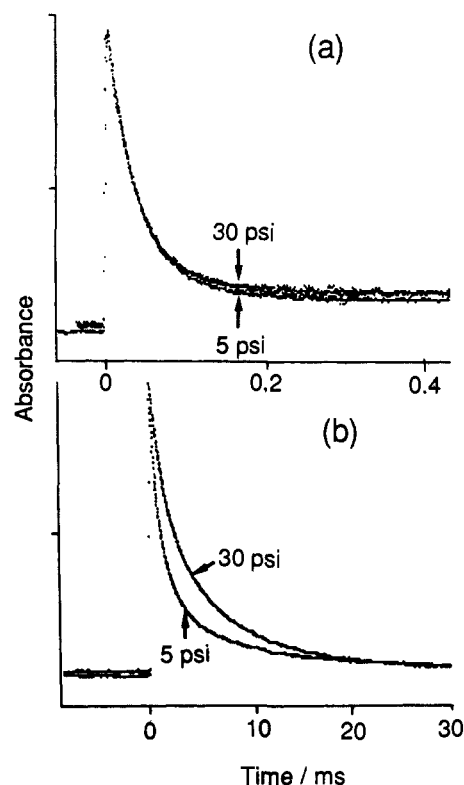


Figure 10. TRIR kinetic traces, showing the lifetime of *fac*-(NBD)M(CO)₃(H₂) depends on the pressure of H₂ above the solution. Traces were recorded in *n*-heptane at 25 °C under two different pressures of hydrogen (5 and 30 psi). In spectrum (a), M = Cr, monitored at 1900 cm⁻¹, and in (b) M = Mo, also monitored at 1900 cm⁻¹. Although the time scale of the Cr traces is much shorter than that of Mo, one can see clearly the difference in behavior of the two metals as the pressure of H₂ is changed.

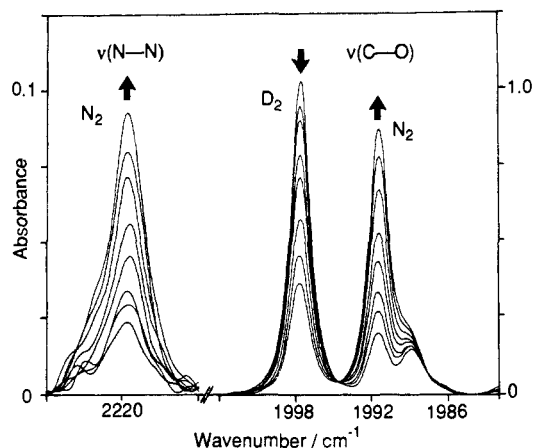


Figure 11. IR bands from the ν (N–N) and ν (C–O) regions showing the thermal reaction of *fac*-(NBD)Mo(CO)₃(D₂) with N₂ (130 psi) in LXe at –91 °C. The bands are marked as follows: D₂, *fac*-(NBD)Mo(CO)₃(D₂); N₂, *fac*-(NBD)Mo(CO)₃(N₂). Note the isosbestic point between the bands of the two species. The spectra were recorded over a period of 14 hr after the venting of D₂ and the addition of N₂.

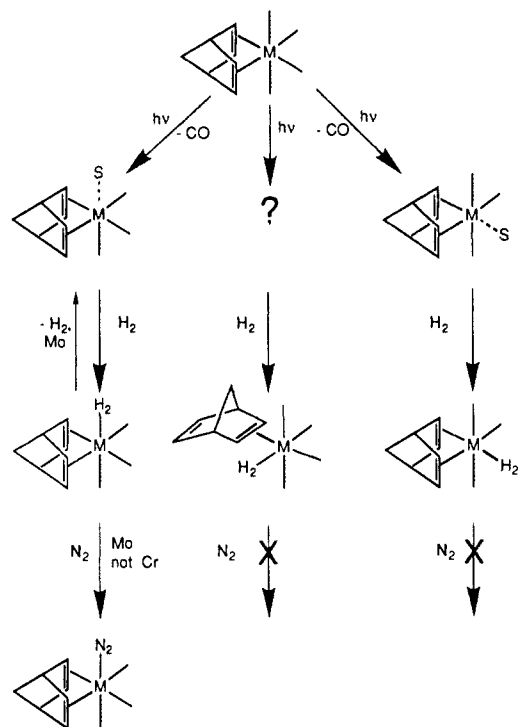
psi pressure of D₂ at –90 °C. After approximately half the compound had decayed, the D₂ was vented, but the rate of decay was unaffected. This suggests that *mer*-(NBD)Cr(CO)₃(D₂) decays by a pathway that does not involve the dissociative loss of D₂.

The thermal reaction of these species with N₂ in LXe is also revealing. As expected the nonclassical complex *fac*-(NBD)Mo(CO)₃(D₂) decays thermally into its N₂ analogue. The decay of the D₂ and growth of the N₂ complexes are shown in Figure 11, including an isosbestic point between the bands of the D₂ precursor and the N₂ product.⁴² Surprisingly, the ν (C–O) bands

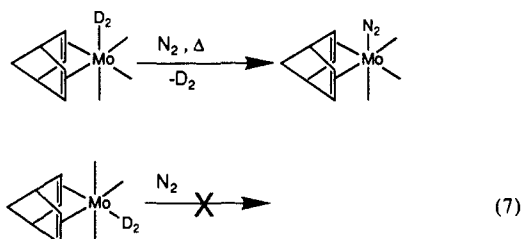
(39) This experiment with W was the only one in which we found evidence of deuteration; a weak band at 2179 cm⁻¹, due to deuterated NBN (for assignments of this band, see ref 1), was detectable at the end of the experiment. Andrea et al.³³ observed similar bands in their experiments with Cr. Given the wavelength sensitivity of these systems, it is possible that the difference between their experiments and ours lies in differences in the photolysis lamps.

(40) This principle has been exploited by use of very high pressures of H₂ to extend the lifetime of dihydrogen complexes at room temperature in both conventional^{6c} and in supercritical solvents (Poliakoff, M.; Howdle, S. M.; Healy, M. A.; Whalley, J. M. *Proc. Int. Symp. Supercritical Fluids* **1988**, 967. Howdle, S. M.; Poliakoff, M. *J. Chem. Soc., Chem. Commun.* **1989**, 1099). For *cis*-(η^2 -NBD)Mo(CO)₄(D₂), there is another decomposition pathway (the intramolecular displacement of D₂ by the uncoordinated C=C bond to give (η^4 -NBD)Mo(CO)₄), the rate of which might be independent of the pressure of D₂.

(41) Unfortunately, *mer*-(NBD)Mo(CO)₃(H₂) is too stable for a similar TRIR experiment to be performed; under ambient conditions $t_{1/2} > 100$ ms, too slow for our TRIR apparatus to monitor and too fast to follow reliably with FTIR.

Scheme IV^a^a M = Cr, Mo

due to *mer*-(NBD)Mo(CO)₃(D₂) and (η²-NBD)Mo(CO)₄(D₂) remain relatively unchanged during the thermal reaction of the *fac* isomer. Unlike the photochemical reaction, there is no evidence for the formation of any N₂ product other than *fac*-(NBD)Mo(CO)₃(N₂) in the thermal process (cf. Figure 8, parts a and c) (eq 7). This suggests that both *mer*-(NBD)Mo(CO)₃(D₂) and (η²-NBD)Mo(CO)₄(D₂) decay by routes which do not involve loss of η²-D₂.



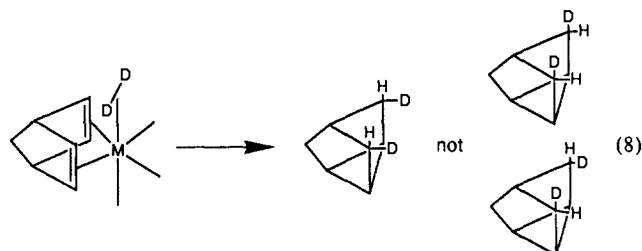
Neither of the analogous Cr complexes, *fac*- and *mer*-(NBD)Cr(CO)₃(D₂), appear to react thermally with N₂ in LXe. Although *fac*-(NBD)Cr(CO)₃(D₂) can only be observed in IR spectra recorded during UV photolysis, no *fac*-(NBD)Cr(CO)₃(N₂) can be detected when the photolysis has ended and the η²-D₂ complex has decayed. This is especially striking because *fac*-(NBD)Cr(CO)₃(N₂) is thermally stable under these conditions (Table V), and one would expect dinitrogen species to be formed by reaction with trace impurities of N₂ (cf. Figure 4). Furthermore, when the labile ethene complex *fac*-(NBD)Cr(CO)₃(C₂H₄) is generated under similar conditions in LXe,¹ it reacts thermally with N₂ to give *fac*-(NBD)Cr(CO)₃(N₂), as expected.

Discussion

The experiments described above have revealed a surprisingly complex set of photochemical reactions between (NBD)M(CO)₄ (M = Cr and Mo) and H₂. The most important of these reactions are summarized in Scheme IV. Two points are important for understanding the photocatalytic hydrogenation of NBD: (i) there

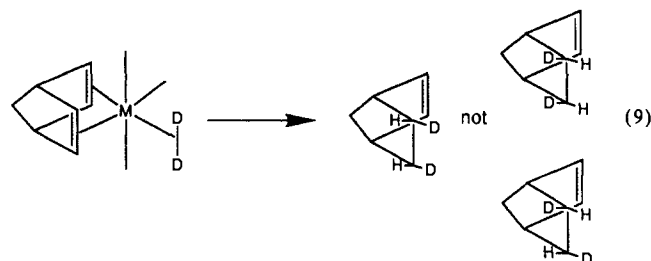
is positive evidence for the formation of three distinct nonclassical dihydrogen complexes, each with NBD also coordinated to the metal center, and (ii) there is no evidence for the formation of any dihydride species. Clearly the crucial stage of the catalytic hydrogenation is the transfer of H₂ to the C=C bond. Although we have not observed this step, we have observed catalytic hydrogenation under the conditions of our experiments (see our second paper¹ for a more detailed discussion). In addition, the thermal behavior of (NBD)M(CO)₃(H₂) (M = Cr and Mo) is consistent with these species decaying by hydrogenation of NBD (see above). It is the purpose of this section to propose a mechanism for the hydrogenation of NBD based on these nonclassical dihydrogen complexes. We show that these proposals offer simple explanations for a number of published observations which, until now, have been difficult to rationalize. We consider the formation of NTC and NBN individually.

(a) **Formation of Nortricyclene (NTC).** We propose that NTC is formed by intramolecular transfer of H₂ to NBD in *fac*-(NBD)M(CO)₃(H₂) (eq 8). The geometry of the *fac*-(NBD)-



M(CO)₃(D₂) would be expected to lead to the endo stereochemistry of deuteration, just as observed by Platbrood et al.^{2b} (eq 8). NTC is a minor product⁴³ with a Mo catalyst but the major product with Cr. This behavior can be understood in the light of our observations that *fac*-(NBD)Mo(CO)₃(H₂) decays largely by loss of H₂ but *fac*-(NBD)Cr(CO)₃(H₂) does not.

(b) **Formation of Norbornene (NBN).** We propose that NBN is formed by intramolecular transfer of H₂ cis to a coordinated C=C bond of NBD (eq 9). Again, the intramolecular transfer of an η²-D₂ group would explain the observed stereochemistry of deuteration.^{2b} *Mer*-(NBD)Mo(CO)₃(H₂) definitely has the re-



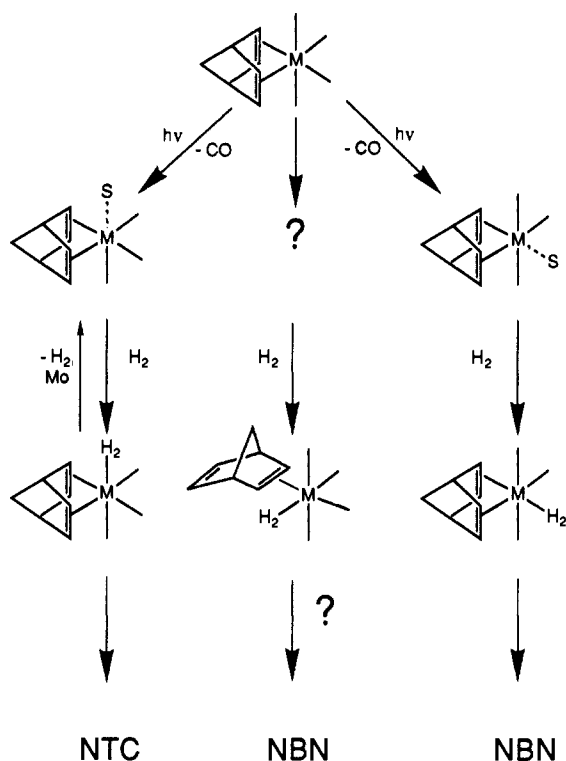
quired geometry for this transfer of H₂, and the same is probably also true of *cis*-(η²-NBD)Mo(CO)₄(H₂). Our results suggest that both of these compounds decay by pathways that do not involve loss of H₂. Thus we cannot distinguish between these two complexes⁴⁴ as the source of NBN, but, given that we have observed no η²-NBD complexes of Cr, we favor *mer*-(NBD)M(CO)₃(H₂).

(43) It has been shown (Mirbach, M. J.; Phu, T. N.; Saus, A. *J. Organomet. Chem.* **1982**, 236, 309) that, with Cr catalysts, NBD can be fully hydrogenated, under a high pressure of H₂, to give norbornane (NBA). The formation of NBA appeared to be at the expense of NTC, suggesting that the two hydrogenation processes were competitive. In our experiments with LXe doped with N₂, we detected secondary photoproducts containing two dinitrogen groups, (NBD)M(CO)₂(N₂)₂. It is possible that, under a high pressure of H₂, the complex (NBD)M(CO)₂(H₂)₂ might be generated. This complex could then lead to NBA by transfer of the two η²-H₂ groups to NBD. A bis-dihydrogen complex would most probably be produced by photolysis of *fac*-(NBD)M(CO)₃(H₂). Since NTC is also postulated to originate from *fac*-(NBD)M(CO)₃(H₂), one would expect the production of NBA to be accompanied by a decrease in the quantity of NTC.

(44) An (η²-NBD)Mo(CO)₄ intermediate was of course proposed by Darensbourg,³ see Scheme 1. Our proposal differs from his in that the compound contains η²-H₂.

(42) The decay of *fac*-(NBD)Mo(CO)₃(D₂) follows pseudo-first order kinetics, and the complete reaction takes ca. 14 h at -91 °C under 130 psi pressure of N₂.

Scheme V

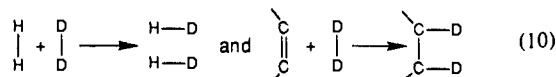


It is quite possible, however, that both routes are important particularly in view of the wavelength dependence of the reaction.

Nonclassical dihydrogen complexes are not unprecedented in catalysis and hydrogenation. Recent examples have included the postulated involvement of nonclassical complexes in hydrogenase and nitrogenase,⁴⁵ and, most recently, a dinuclear complex has been shown to transfer H₂ to hexene.⁴⁶ The transfer of an η²-H₂ group to an olefinic C=C bond in a *cis*-(η²-H₂)(olefin)ML₄ complex has considerable similarities to the H/D isotopic scrambling which we have previously reported^{6c} for *cis*-(η²-H₂)(η²-D₂)Cr(CO)₄ (eq 10). This H/D exchange since has been the subject of considerable theoretical interest.^{6f,g}

(45) Crabtree, R. H. *Inorg. Chim. Acta* **1986**, *125*, L7.

(46) Hampton, C.; Cullen, W. R.; James, B. R. *J. Am. Chem. Soc.* **1988**, *110*, 6618.



These reactions can now be combined with our photochemical observations to give an overall mechanism for the hydrogenation (Scheme V). The crucial difference between this scheme and all previous proposals^{2,3} is that we have positive evidence for the existence of the proposed intermediates and that nonclassical dihydrogen complexes are proposed as the catalytically active species.

Conclusions

The experiments reported here show that d⁶ metal centers form nonclassical dihydrogen complexes rather than dihydrides under the conditions in which photocatalytic hydrogenation of dienes occur. The photolysis of a range of NBD and ethene complexes in the presence of H₂ generates nonclassical dihydrogen complexes without any evidence for the formation of dihydride species. These nonclassical compounds have been detected not only in liquid Xe at low temperature (FTIR) but also in *n*-heptane under ambient conditions (time-resolved IR). Our results show that these species can exist under the conditions of photocatalysis and may well play an important part in the catalytic cycle. Scheme V summarizes the proposed role of these complexes in the hydrogenation of norbornadiene (NBD). The most significant feature of these proposals is the intramolecular transfer of H₂ to the C=C bond. Such a transfer provides a simple explanation for the observed stereochemistry of the addition^{2b} of D₂ to NBD.

This paper has concentrated largely on the role of dihydrogen in these reactions and has illustrated the value of focusing several spectroscopic techniques on the same mechanistic problem. In our second paper,¹ we present experimental evidence, particularly kinetics, for the role of the diene in these reactions and then propose a rather fuller scheme for the catalytic cycle.

Acknowledgment. We are grateful for support for EEC (Stimulation Contracts No. SC1*0007 and ST2*/00081), SERC, NATO (Grant No. 741/85), the Paul Instrument Fund, the Petroleum Research Fund, administered by the American Chemical Society, Nicolet Instruments Ltd., and Applied Photo-physics Ltd. M.P. thanks the Nuffield Foundation for a Research Fellowship. We thank Dr. A. J. Rest for permission to quote his unpublished matrix isolation data. We thank J. M. Whalley for his technical assistance and the many people who have discussed these results with us, particularly Professors J. K. Burdett and J. A. Connor and Drs. M. A. Healy, W. E. Klotzbücher, B. P. Straughan, and R. Whyman.